No 727481 RESERVE
D5.2 v1.0
Report on field trial of voltage control concepts in Ireland and validation of initial network codes and ancillary service definitions

The research leading to these results has received funding from the European Union's Horizon 2020 Research and Innovation Programme, under Grant Agreement no 727481.

Project Name	RESERVE
Contractual Delivery Date:	30.09.2018
Actual Delivery Date:	29.09.2018
Contributors:	RWTH, TSSG, ESB, UCD
Workpackage:	WP5–Field trial of voltage control concepts
Security:	PU
Nature:	R
Version:	1.0
Total number of pages:	51

Abstract
This document focuses on implementation of the RESERVE field trials at three trial sites as well as in the laboratory at RWTH in Aachen, Germany. The field trial sites will perform different tests designed to test the implementation of voltage management solutions under a range of conditions. The laboratory configuration at RWTH will integrate all RESERVE Components as they become available and will perform tests on the entire solution. This document also describes contribution of the RWTH laboratory to the tests performed at the remote trial sites. Finally, the Voltage control solutions are presented.

Keyword list
Integrated Grid, Smart Grid, field testing, laboratory testing, AVM, VOIP, DVSM, VOIP

Executive Summary

This deliverable describes progress to date with regard to the preparation and delivery of infrastructure and associated systems to demonstrate the deployment in the field of voltage control concepts developed within the RESERVE project.

The delivery of Field Trials can be categorized into two broad divisions namely;

A. Trials associated with the Dynamic Voltage Stability Margin (DVSM) Control Technique

B. Trials associated with the Active Voltage Management (AVM) Control Technique

A. In order to trail the performance of the DVSM Control Technique a new class of inverter is being developed due to the inability of existing commercially available inverters to perform the required functions of Wideband System Identification (WSI) and Virtual Output Impedance (VOI) Control. The first prototype of this new inverter is currently under test with release for real time laboratory-based test simulations expected in the coming months. This will be followed by trials in the field at a facility located in Portlaoise, Ireland. A test plan for these trials is set out in this document which includes proposals to test and verify a number of new Network Code proposals developed in the RESERVE project.

B. In relation to the development of trial site infrastructure related to the Active Voltage Management (AVM) control technique a total eight field trial locations have been delivered in Ireland, each equipped with one of a number of relevant inverter-based technologies including Solar PV Installations, a Vehicle to Grid (V2G) Charging System and Domestic Scale Battery Systems. Integration of the trial sites from an ICT perspective has involved the development of components, both hardware and software, that enable communication between the trail sites and cloud components and also platforms and applications that cache, receive and execute the Active Voltage Management technique. With regard to the AVM technique itself, a brief overview of the proposed decentralized active voltage management algorithm is provided. The proposed AVM algorithm is then applied to extract the VVCs for several trial sites of RESERVE project for static voltage stability analysis.

Overall the report details the significant strides which have been made in the period since the delivery of D5.1 in constructing the trail site facilities, developing appropriate ICT interfaces to each site and in applying the theory for voltage control developed in RESREVE to locations which are subject to an array of electrical configurations and cutting-edge inverter based technologies. The progress has placed this element of the project in a good position to deliver robust testing of the control techniques whilst also allowing scope for further refinement and detailed evaluation of their technical and economic benefits before the project's conclusion.

Authors

Partner	Name	Phone / Fax / e-mail
RWTH	Sriram Gurumurthy	sgurumurthy@eonerc.rwth-aachen.de
	Markus Mirz	Mmirz@eonerc.rwth-aachen.de
TSSG	David Ryan	dryan@tssg.org
	Miguel Ponce de Leon	miguelpdl@tssg.org
	Niall Grant	ngrant@tssg.org
	Rachael Lawton	rlawton@tssg.org
ESB	Jonathan Sandham	jonathan.sandham@esb.ie
	Ronan Murphy	ronan.murphy@esb.ie
	David Fogarty	david.fogarty@student.esb.ie
UCD	Alireza Nouri	alireza.nouri@ucd.ie
	Alireza Soroudi	alireza.soroudi@ucd.ie
	Andrew Keane	andrew.keane@ucd.ie

Table of Contents

1. Introduction

1.1 Scope of the Deliverable

RESERVE focuses on the energy systems at the system level, based on novel research concepts virtualising the control of power networks and on the use of a ground-breaking new pan-European real time simulation platform for the large-scale simulation of potential new solutions.

The document D5.2 is the second deliverable associated with the delivery of Field Trials for Voltage Control Scenarios within the RESERVE project and builds upon the findings in D5.1. It contains information about the design, installation, commissioning, execution and operation of the field trial sites in Ireland.

1.2 How to read this Document

Before reading this document, the reader should read the document D1.1 which motivates the RESERVE project, describes the architecture of the RESERVE system and describes the RESERVE proposition, which instantiates the various architectures. We will avoid repeating detailed descriptions, which may be found in D1.1 and D1.4. Furthermore, documents D3.3 for stability monitoring algorithm, D3.4 for WSI, D3.5 for VOI calculation and overall system level control, D3.6 for ICT requirements may also be of benefit to the reader.

1.3 Summary of Work Completed to Date

1.3.1 Preparation for Dynamic Voltage Stability Margin (DVSM) Field Trial

To test the algorithms proposed in the scenario Dynamic Voltage Stability Monitoring (Sv_A), a new class of inverters are required. In the impedance-based approach undertaken in Sv_A, the measurement of grid impedance is a crucial step. A wideband system identification (WSI) tool is developed to measure and extract the grid impedance by injecting small signal perturbations in the control of the inverter. The process of procuring such new class of inverters which does not exist in the market, externally, was not cost effective. Therefore, RWTH is developing a new inverter with the proposed functionalities of WSI and virtual output impedance (VOI) control algorithms. The inverter prototype can be subdivided into 2 parts: power board and measurement board. The power board comprises of the power electronic switches, gate drivers and power filters. On the other hand, the measurement board hosts the analogue circuitry for high bandwidth current and voltage sensing. Currently, the circuit schematic of both the power boards and measurement boards are complete. Furthermore, the PCB layout of the measurement board has been completed and the testing and commissioning of the first prototype is ongoing. Preparation of PCB layout for the power board is in process. Fully tested first prototype is expected to be completed by M26. This will be followed by trials in the field at a substation facility located in Portlaoise, Ireland.

1.3.2 Preparation of Active Voltage Management (AVM) Field Trial Sites

The development of Field Trial locations in Ireland in which to test the viability of the AVM Voltage Control Technique in a number of real world environments has continued apace over the past year. All eight field trial installations have now been completed, commissioned and energised. Each installation comprises an inverter-based technology which has a specific application related to generation, storage or usage of electrical energy. The completion of these installations will now facilitate the rigorous testing of the AVM technique over the remaining 12 months of the RESERVE project.

1.3.3 Tuning of the AVM Control Technique for each Specific Field Trial Site

In subsection 3.2, a brief overview of the proposed decentralized active voltage management algorithm is provided. More details on this algorithm can be found in D3.2 to D3.5. The proposed AVM algorithm is then applied to extract the VVCs for several trial sites of RESERVE project for static voltage stability analysis (SV_B). The definition of SV_B is given in D1.5. The ESB trial sites include RES-PV-NTC-0, RES-BAT-FIRE-0 and RES-V2G-LEOP-0, located at Portlaoise (ESBN National Training Centre (NTC), Portlaoise), Ballyvolane Fire Station (North Ring Road, Ballyvolane, Cork), and Leopardstown V2G Charge (ESBN Offices, Leopardstown, Dublin) were used to validate the proposed decentralized active voltage management algorithm for inverter based solar PV array, battery storage and V2G systems, respectively.

1.3.4 ICT Trial Site Integrations and Communications

The integration of the trial sites from an ICT perspective has involved the development of components, both hardware and software, that enables communication between the trail sites and cloud components and also platforms and applications that cache, receive and execute the Volt-VAR Curve which is the output of the Active Voltage management technique (Sv_B). Some of these components are generic to all the trial sites and some are specialist interfaces that enable direct communication with the RES Unit. Each trial site implementation is at a different stage in terms of integration from an ICT perspective and detailed briefly below is a status on each.

- The Battery Trial Site in terms of implementation is the most advanced as in we are receiving data and calculating the Reactive Power Setpoint and sending it to the trial site for injection into the inverter.

- For the V2G trial site we have decided on the method of communication and a hardware component has been developed with the relevant bespoke software to execute the VVC installed.

- Currently the Solar PV integration is in the investigative stage and we have decided on a communications model and have an implementation plan developed in terms of the execution of the VVC.

2. Virtual Output Impedance Field Trials

This chapter consolidates the preparatory activities undertaken in the realisation of virtual output impedance field trials and the simulation plans undertaken to validate network codes.

2.1 Introduction and Background

To test the algorithms proposed in the scenario Dynamic Voltage Stability Monitoring (Sv_A), a new class of inverters are required. In the impedance-based approach undertaken in Sv_A, the measurement of grid impedance is a crucial step. A wideband system identification (WSI) tool is developed to measure and extract the grid impedance by injecting small signal perturbations in the control of the inverter. The process of procuring such new class of inverters which does not exist in the market, externally, was not cost effective. Therefore, RWTH is developing a new inverter with the proposed functionalities of WSI and virtual output impedance (VOI) control algorithms. Fully tested first prototype is expected to be completed by M26.

Goal of the Irish field trial is to measure the grid impedance with the proposed prototype inverter and examine the quality of extracted impedance. Validation of the inverter prototype and its impedance measurement capabilities in the Irish test grid will enable further validation of concepts and network codes pertaining to Sv_A scenario through the trials in Aachen Lab.

2.2 Theory

2.2.1 Impedance based stability for active distribution grids

The phenomenon of harmonic instability and parallel resonance has been mapped to the concept of impedance from the Middlebrook theory. The stability properties of a power-electronic driven system can be adjudged by the impedance ratio of the grid as seen from the converter and the converters impedance. Thus, the proposed Dynamic Voltage Stability Monitoring (Sv_A) technique starts from the measurement process: the grid impedance as seen from the RES inverter needs to be measured. An online non-invasive technique based on Wideband System Identification (WSI) for the grid impedance measurement is reported in Deliverable D3.4. Real-time hardware-in-the-loop simulations show the effectiveness of the WSI technique to measure and estimate the grid impedance.

2.2.2 Virtual Output Impedance (VOI) control

Closed loop impedance of the inverter is dependent on the control loops of the inverter. Modifying the controller changes the impedance of the converter. Control techniques in literature which try to modify the output impedance do not consider the real-time grid impedance. From the Middlebrook theory and its advancements, it is proved that the stability of every power electronic interface is dependent on the ratio of the grid impedance and inverter output impedance. The VOI technique proposed in WP3 considers the real-time grid impedance data for the synthesis of stabilising VOI controller. Real-time measurements of the impedance through the WSI tool enables the application of advance control techniques such loop-shaping techniques for the synthesis of VOI. Ultimately, the impedance of the inverter is modified to suit the measured grid impedance. Concept of VOI is illustrated in **Fehler! Verweisquelle konnte nicht gefunden werden.**. Details of the VOI controller and its synthesis can be found in Deliverable D3.5.

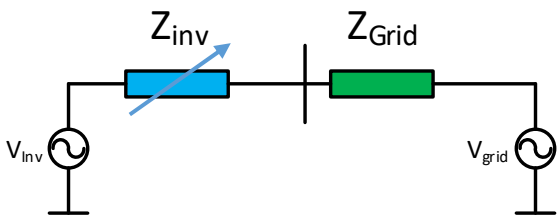

Figure 1 VOI Concept

2.3 Data Information Systems & Software Implementation

The Secondary Substation Automation Unit (SSAU) will host the dynamic stability monitoring algorithm and acts as a coordinator to extract local impedance information from every inverter. A wideband system identification (WSI) tool is required to measure the impedance spectrum online. A Psuedo Random Binary Sequence (PRBS) signal is injected in the inverters controller which perturbs the inverter output voltages and currents for a very short period of time (20-200 ms). The perturbed voltages and currents are stored in a FIFO buffer in the inverter's controller. The WSI tool can extract impedance spectrum out of this time domain data stored in the FIFO buffer.

2.3.1 WSI implementation

Due to the computational complexity of the WSI tool, we consider 2 options for implementing the WSI tool.

2.3.1.1 WSI algorithm implemented locally at the inverter controller

- The controller of the inverter has the complete WSI algorithm. This includes the subroutines like PRBS noise generation, extracting the non-parametric impedance and parametric impedance identification.
- The Inverter uses communication to communicate only the identified impedance coefficients. Communication data volume is low.

2.3.1.2 WSI algorithm implemented centrally in SSAU

- The controller of the inverter has only the PRBS noise generation subroutine.
- The rest of the WSI functionalities such as extracting the non-parametric impedance and parametric impedance identification is performed in SSAU.
- The Inverter uses communication to send voltage and current data measured during the perturbation. Communication data volume is high.

Deliverable D3.4, D3.5 and D3.6 can be referred for depth in details for implementation and ICT aspects respectively.

2.3.2 Stability Monitoring Algorithm and VOI calculation

The stability monitoring algorithm and the VOI control calculation will be implemented in the SSAU. The description of these algorithm can be found in D3.3 and D3.5.

2.4 Trial Site Implementation

2.4.1 Low power inverter prototype development

The ratings of the developed low power inverter prototype are given in **Fehler! Verweisquelle konnte nicht gefunden werden.**. A modular design is adopted to save space and reduce the time and cost in case of replacement. The LCL filter and measurement boards are modularised and they can be stacked onto the main inverter board. This allows the inverter to be dismantled into individual PCBs.

Parameter	Values
Rated Power	300 W @ 50 kHz
Switching frequency	50 kHz
DC Link Voltage	700 V-750 V
Grid line voltage and frequency	400 V, 50 Hz
Converter side choke (L_c)	2.7 mH
Grid side choke (L_g)	1.8 mH
Filter capacitance (C_d and C_f)	0.5 µF and 0.5 µF
Damping resistor	300 Ω

Table 1 Parameters of the low power prototype

2.4.1.1 Inverter and power filter board

Functional block diagram of Inverter is shown in Figure 2. The semiconductor switches and the gate drive logic are realized from the intelligent power module (IPM) technology-based integrated circuit FSBB20CH120D by ON Semiconductors. Considering an operating power of 300W, the inverter can be operated with a switching frequency of 50 kHz. However, when the inverter needs to be operated at a much higher power, then the switching frequency can be reduced to 20 kHz or 15 kHz to be in safe operating mode. This IPM offers inbuilt short circuit current protection and galvanic isolation. The control signals that drive the PWM and relays are provided from the Labview NI FPGA controller. Digital isolator ICs are incorporated in the design to protect the Labview NI FPGA from the high voltage side.

The power filters are realized with an LCL filter with split RC damper to suppress the filter resonance. Relays are included to configure the power filter (i.e LC or LCL) and to configure the shunt damper. The cut off frequency of the LCL filter is designed to be roughly one tenth of the switching frequency. Since the inverter is planned to be operated at 50 kHz, the cut off frequency of the realised filter is 5.01 kHz. A split capacitor damping topology is realized for the passive damping circuit. Objective of the damper is to remove the resonance peak introduced by the LCL filter at its cut-off frequency.

Currently the schematics are completed, and PCB design is on progress. Expected completion of the first tested prototype is by M26.

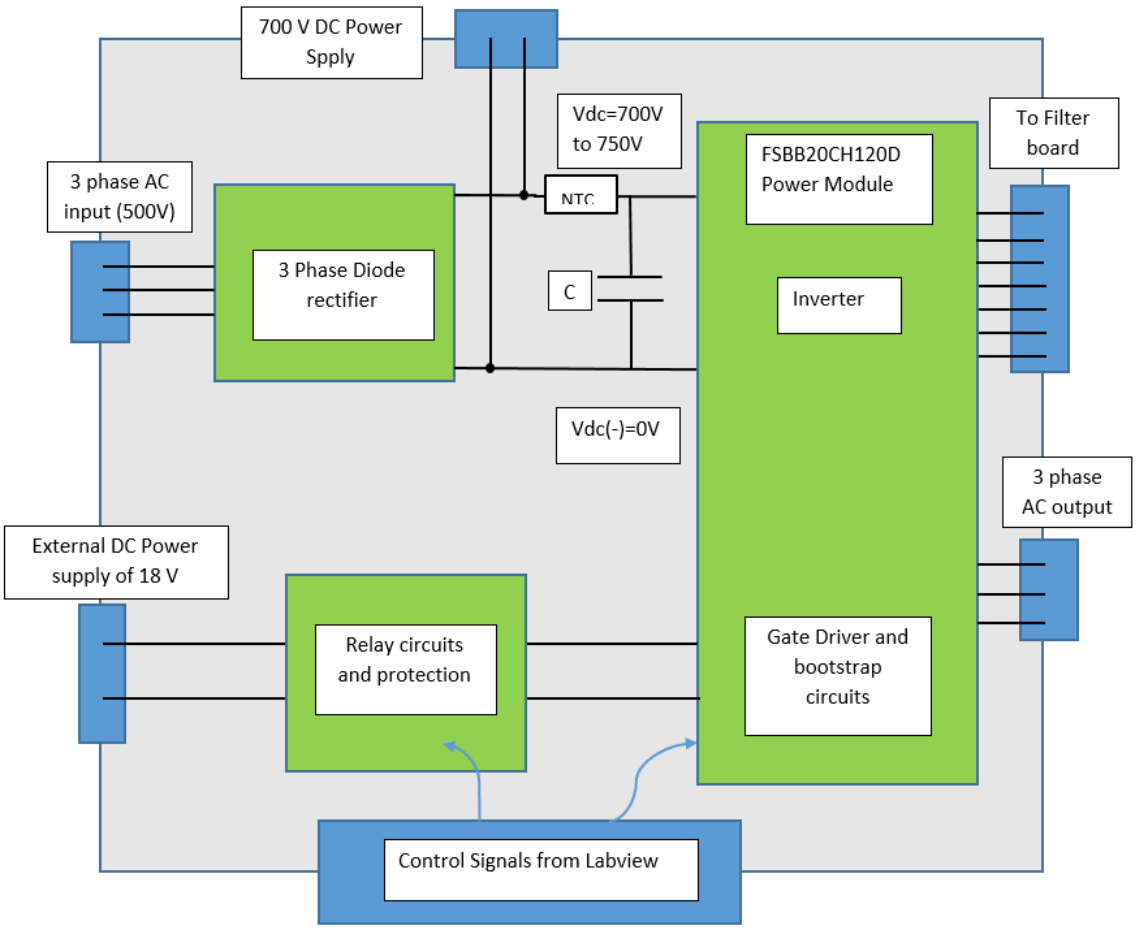

Figure 2 Inverter Board - Functional block diagram

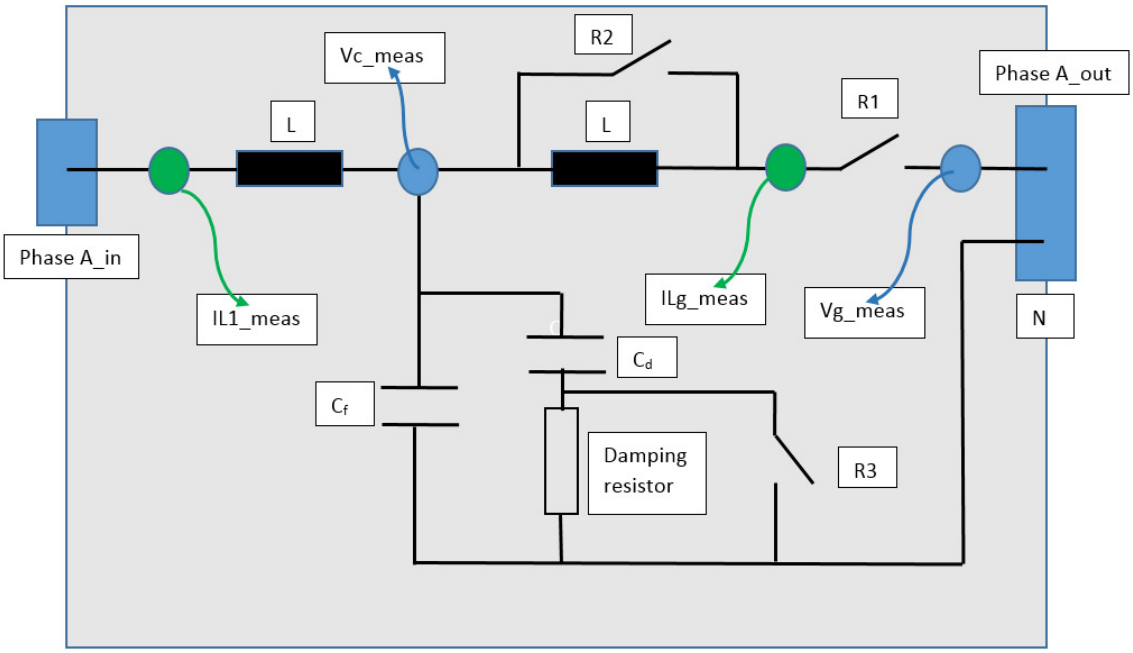

Figure 3 Filter board (per phase) - Functional block diagram

2.4.1.2 Measurement board

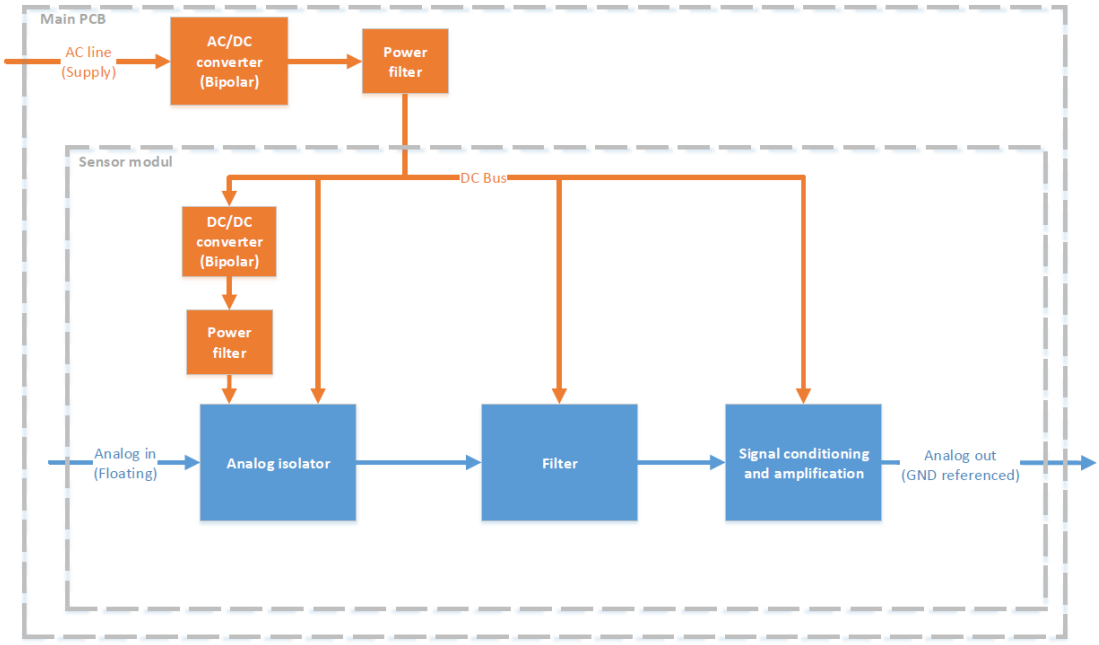

Figure 4 Measurement board - Functional block diagram

Functional Block Diagram of measurement board is shown in Figure 4 and the first prototype of the built measurement board is shown in Figure 5. The developed measurement board can be used for both current and voltage measurements. During the PRBS noise injection stage, the perturbations could be injected at a rate close to the switching frequency of the inverter. To measure the perturbed line currents and phase voltages (line-neutral voltage); a high bandwidth, low distortion measurement board is required. Furthermore, due to the presence of high voltages in the neighbourhood (such as LCL filter components), appropriate galvanic isolation is required. The proposed measurement board satisfies the above-mentioned constraints. It is tested to have an excellent bandwidth and offers a galvanic isolation of 5kV. Phase currents up to 5A, DC side voltage of 1000V and AC side phase voltages of 550V can be measured with the proposed high bandwidth measurement board.

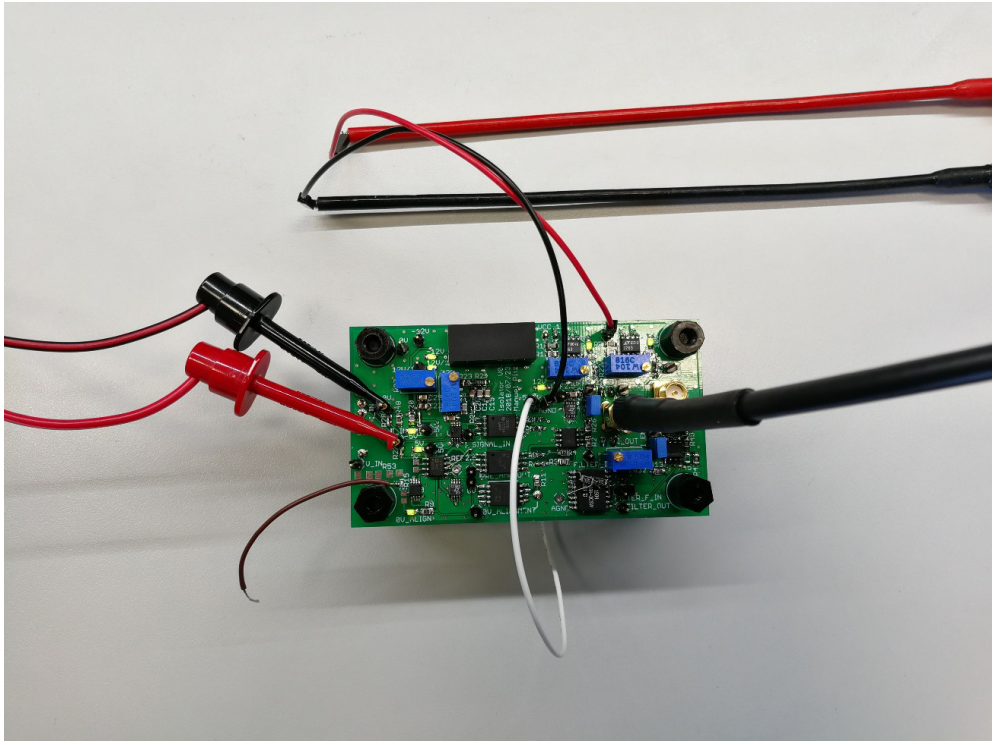

Figure 5 High bandwidth measurement board

2.4.1.3 Control algorithm

The control algorithm is implemented in a Labview real time FPGA target. The control algorithm in the inverter can be grouped in 2 parts: Operation&Control and Impedance measurement.

Operation&Control: A cascaded proportional-integral (PI) control is implemented for controlling the grid injected current. Additionally, the proposed VOI loop is included in into the cascaded structure. This group also contains all the signals to operate the relays.

Impedance Measurement: Contains the WSI tool and its components.

2.4.2 ESB Trial Site Preparation

In order to verify the operation of the new model inverter and the associated AVM control technique in a real world environment a suitable test location has been identified. The test location is located within Burnwood 38 kV GIS station which is located within ESB Networks National Training Centre in Portlaoise, Ireland. Connecting the inverter at this location will subject it to the continuously variable network operational parameters of this active facility and provide a baseline test of it's suitability for further field deployments. In preparation for the inverters deployment to the location suitable additional electrical and ICT connection points have been installed in the facility.

2.5 Test Plans

2.5.1 In-field experiments at ESB, Ireland

The experimental setup to be used in Ireland is shown in Figure 6. The low power inverter prototype is encapsulated within the red box.

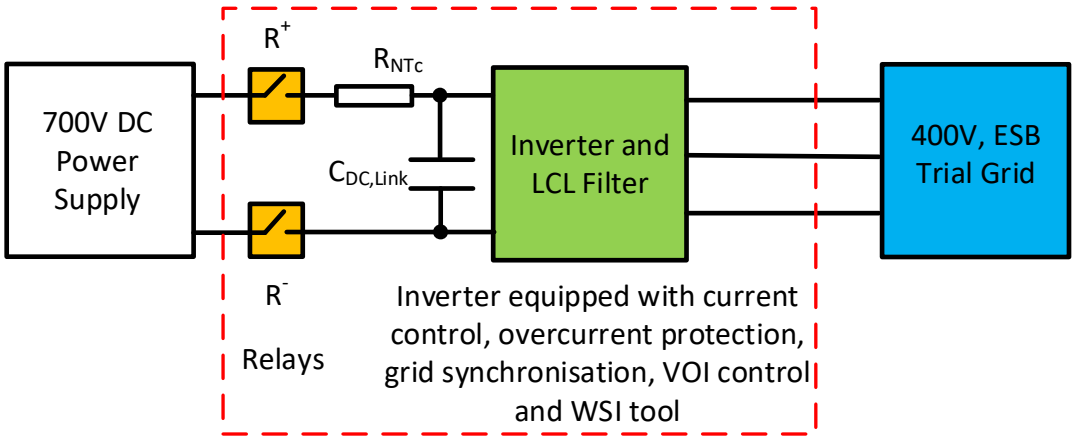

Figure 6 SV_A Field Trial - Hardware Setup

The inverter will be operated in grid connected mode. PRBS noise will be injected for 200 ms (10 cycles) and simultaneously the voltage and current measurements are sampled. This data will be stored in a first-in-first-out (FIFO) buffer;

(A) See the quality of extracted non-parametric impedance.

(B) study the impact of PRBS noise level on the extracted impedance

(C) Optional step - Activate the VOI control loop and observe the performance. This step is mainly applicable for the Aachen Lab Trial.

(D) Save data for future analysis, since we will develop stability analysis and VOI methods based on non-parametric impedance data. Such a data driven method will eradicate the requirement of system identification techniques wherein the system order needs to be predefined or assumed

2.5.2 HiL experiments at RWTH lab, Aachen

Validation of DVSM algorithm will be undertaken in RWTH lab in Aachen using the HiL setup shown in Figure 7. The HiL setup consisting of OPAL-RT and Labview are already running and this setup is used to validate the WSI tool. An extension of this real-time simulation is the inclusion of the virtual machine (VM) where the stability monitoring algorithm and VOI calculations are implemented. This experiment will effectively demonstrate the idea of ICT driven decentralised control in futuristic distribution grids which DSOs can adopt.

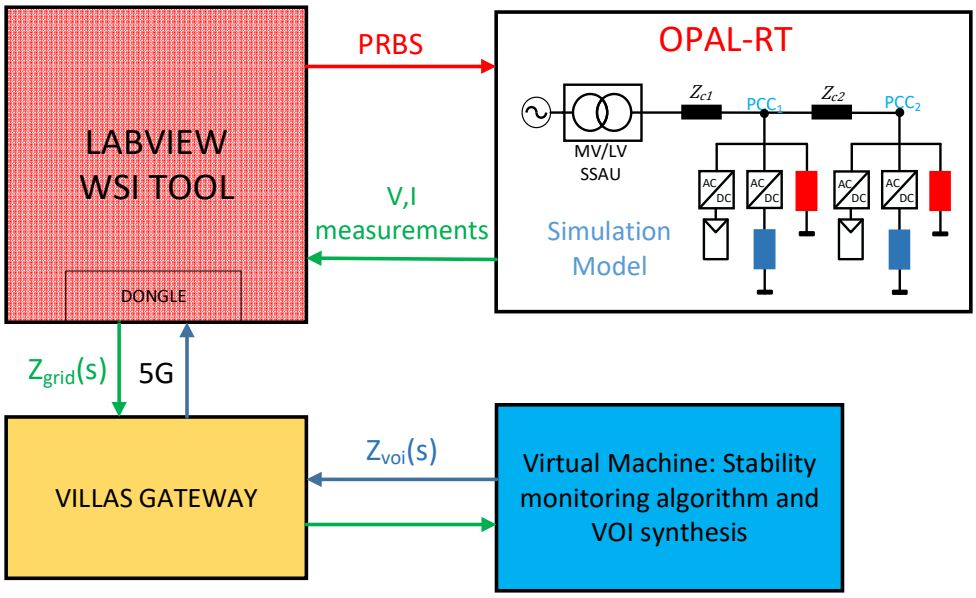

Figure 7 DVSM (SV_A) HiL Validation at RWTH lab, Aachen

Before performing the test in Ireland, a trial will be performed in RWTH lab in Aachen. The setup consists of a low power inverter connected to a passive load as shown in Figure 8 . WSI which is local to the inverter measured the grid impedance, which is the known passive load in this case. The measured grid impedance data is communicated to a virtual machine (VM) which mimics the role of the SSAU. Stability monitoring calculations and VOI calculations will be implemented in the VM.

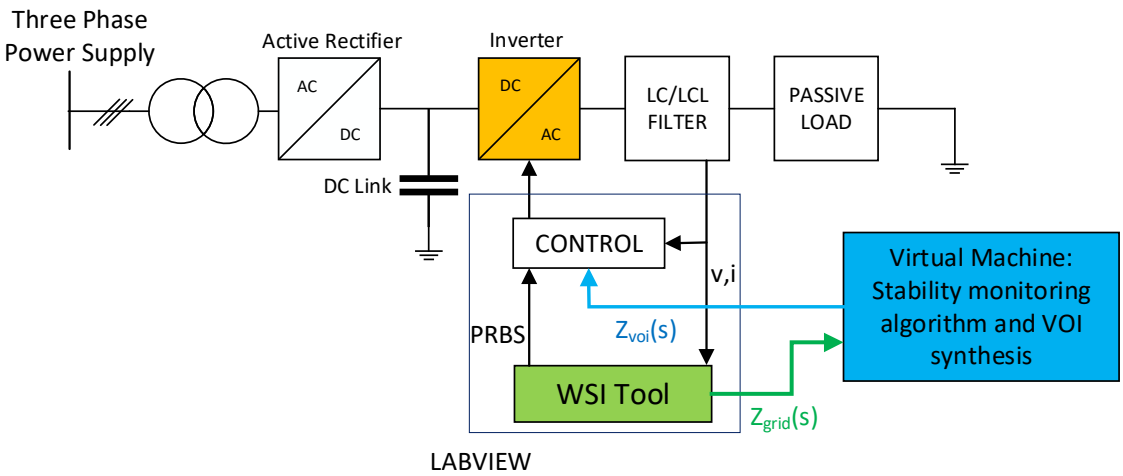

Figure 8 DVSM Field Trial in RWTH lab, Aachen

2.5.3 Grid Codes

One of the main objectives of RESERVE is to map the new techniques to network codes (NC) and ancillary services. By studying the existing NCs for voltage control in distribution systems among various DSOs in EU and by deriving the objectives of the proposed voltage control techniques, proposal for NCs and modifications to existing NCs are made. Over the last 12 months, work has been done to map the simulation scenarios and the field trial experiments to network code validation. The 5 important network codes arising from the voltage control work is given below.

NC.1 Decentralised Voltage Control

NC.2 Leading Power Factor Operation

NC.3 Dynamic Stability Margins

NC.4 Requirements for new behaviour of RES inverters

NC.5 New requirements for the perturbations injected from RES inverters

The mapping between the validation of these codes and planned simulation and trials can be found in D3.8.

2.6 Conclusion

To test the proposed DVSM technique, new class of inverters are currently under development. The first prototype of the measurement boards is currently under test and first tested prototype of the power and filter board will be completed by M26. The mapping between NCs with both simulation scenarios and field trials are completed. Few of the real time simulations are completed and remaining simulations are planned to be completed in the next 6 months. The results of real-time simulations related to WSI tool are reported in D3.4.

3. Active Voltage Management Field Trials

3.1 Background

In contrast to the requirement of the Virtual Output Impedance control technique to develop a new prototype inverter, the Active Voltage Management (AVM) Field Trials can be implemented using existing commercially available inverter technology. Electricity generation and storage technologies are experiencing significant and accelerating demand as the focus on decarbonisation and increased electrification intensifies globally. Many of these new technologies include inverters due to the fact they are coupling DC based devices to external AC networks. This presents a distinct opportunity for the AVM control technique as it can leverage inverter technology that is already being deployed for other purposes without requiring installations purely dedicated to its realisation. Indeed many of the system stability challenges which the AVM technique has been designed to alleviate are themselves exacerbated by a proliferation of new electricity generation and storage installations. Realisation of the AVM technique should both facilitate the installation of these new installations and allow for ever more intensive deployment on existing networks without requiring the level of investment associated with traditional electrical network capacity uprating.

n selecting specific technologies for the AVM Filed Trials, it was decided to mix more established technologies such as Solar PV with more cutting edge technologies such as Vehicle 2 Grid chargers. These selections will allow us to compare and contrast the impact of technologies on the effectiveness of the control technique across a range of network configurations located in both rural and urban environments. All AVM trial sites are located in Ireland connected to low voltage distribution networks which are operated by a single Distribution System Operator, ESB Networks. This has allowed for standardised, connection design, and monitoring and will facilitate consistent analysis of network impact.

3.2 Theory

3.2.1 Synopsis

The details of the proposed active voltage management algorithm was presented in D3.2 to D3.6. The algorithm of obtaining Volt-Var Curves (VVCs) is outlined below:

- Stage 1: determines the optimal voltage across all scenarios that minimises the voltage unbalance of the feeder, or other objectives of interest, considering unlimited reactive power support for all RESs.

- Stage 2: determines the closest possible voltage deviation from optimal in each scenario, constraining the reactive power of the RES units to within representatively realistic bounds.

- In Stage 3: the voltages are determined that occur at varying generation levels coinciding with the voltage sensitivities of demand at these times.

- Finally, to conclude the offline-procedure the resulting reactive power set-points (Stage 2) are plotted against the resulting voltage set-points (Stage 3) to determine the Volt-Var curves for each RES system.

3.2.2 Objective Menu

In the active voltage management of low voltage distribution systems, the main objective depends on the system requirements and also the availability of the controllable devices that can effectively satisfy such objectives. In such systems, the availability of the renewable energy resources and other controllable inverter-interfaced devices, enable the system operator to control the load point voltages more effectively to achieve variety range of objectives. In this

project, three main objectives are considered for the active voltage management in futuristic low voltage distribution systems. These objectives are presented in **Table 2**.

In **Table 2**, the inverter types (three-/single-phase) that can help the system operator (partially) satisfy a specific objective and also the network types in which a specific objective can be followed are presented. It should be noted that the effectiveness of some types of inverters are lower in satisfying some objectives and also in some types of networks. It is also possible that even with all the capacity control available in a network, the network issues cannot be fully resolved.

Code	Objective	Requirements	Three phase Network	Single phase Network
1	Voltage unbalance improvement	Single-phase inverter	✓	X
2	Loss reduction	Both Single/three-phase inverters	✓	✓
3	Improvement of voltage deviation ($V_{desired}$=1 pu.)	Both Single/three-phase inverters	✓	✓

Table 2 Objective Menu

3.2.3 Implementation of VVCs

The capacity of each inverter is limited by the maximum current that the device switches can interrupt or the thermal current limit specified by the manufacturer and also by the maximum inverse bias voltage of the switches or the maximum voltage level that the device insulation can tolerate in steady state condition. In the steady state studies of power systems, these limitations are usually modelled by a single constraint, i.e., the apparent power injected by this inverter cannot be higher than the maximum allowable apparent power which is always referred to as the inverter capacity.

The reactive power support of each inverter unit should be determined considering this limitation. In fact, by measuring the voltage at the connection point of this inverter, the change in the reactive power support provided by this inverter can be found using the regarding VVC. However, it is possible that this change cannot be fully applied due to the apparent power limitation of this inverter. With P_g as Q_g as the active and reactive power injection of the inverters before developing the voltage control strategy and S^{max} as the maximum allowable apparent power of this inverter, the change in the reactive power support (ΔQ_g) should satisfy constraint **(**, where as shown in **(2)**, ΔQ_g+Q_g is the total value of the reactive power injected by this inverter.

$$-\sqrt{\left(S^{\max}\right)^2 - P_g^{\,2}} \le \Delta Q_g + Q_g \le \sqrt{\left(S^{\max}\right)^2 - P_g^{\,2}} \qquad \textbf{(1)}$$

$$Q_g^{total} = \Delta Q_g + Q_g \qquad \textbf{(2)}$$

Therefore, the change in the reactive power support should be found using the following steps to satisfy the inverter capacity constraints. In these steps, Q_g^{final} is the final value of the reactive power support that this inverter should provide.

1) Find the optimal change in the reactive power support of this inverter, i.e., ΔQ_g^{opt} using VVCs extracted in offline simulations.
2) If $Q_g^{total}=Q_g+\Delta Q_g^{opt}$ is between the upper and lower limits presented in (, set Q_g^{final} to Q_g^{total}.
3) If $Q_g^{total}=Q_g+\Delta Q_g^{opt}$ is greater than the upper limit (, set Q_g^{final} to the upper limit proposed by (.
4) If $Q_g^{total}=Q_g+\Delta Q_g^{opt}$ is lower than the lower limit (, set Q_g^{final} to the lower limit proposed by (.

It should be noted that other than capacity constraints, some other limitations may be applicable in the operation of special types of controllable devices. Such limitations were reviewed in **D3.3** and were applied in the case studies of that deliverable. In that case, this limitations should be taken into account in calculation of the upper and lower bounds on the reactive power support of each inverter.

3.3 Data Information Systems & Software Implementation

In discussing the data information systems and software implementation from a trial site perspective it is first worth mentioning that there is a diverse nature of the entities at each trial site. This diversity includes the communications medium, control mechanism, end device capabilities and environmental factors. Therefore, the implementation of the AVM algorithm execution in terms required components, deployment, location of execution and data transfer all have different properties and configurations.

These diversities and the ICT requirements for each trial site have been catered for in a set of architectures detailed in D3.6 section 3.1.2, where they are categorised as Centralised, Decentralised and Hybrid Edge Computing. While there are diversities on a site by site basis the main functions all remain the same. These functions include data access, algorithm execution and device control based on the output of the algorithm execution. The specific details of how these functions are carried out for each site are detailed in section 3.4.

3.4 Trial Site Implementations

3.4.1 Vehicle to Grid (V2G) Charger Installation

3.4.1.1 Background

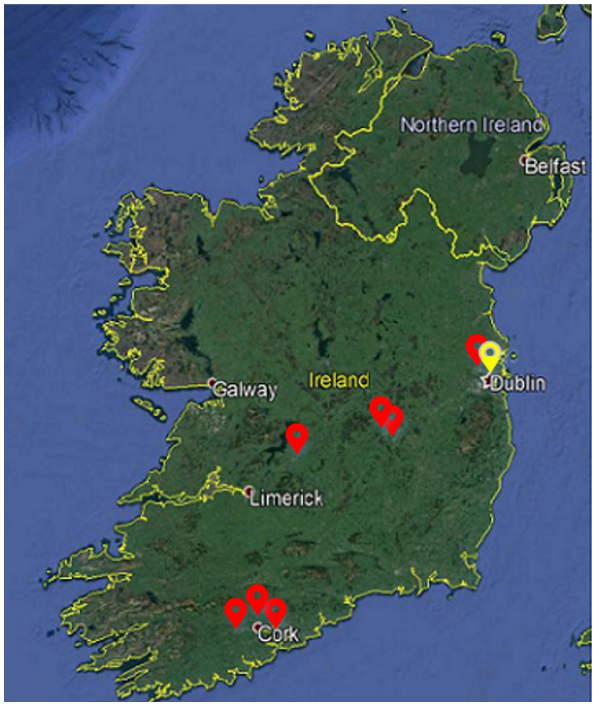

Figure 9 Location of V2G Charger Trial Site

A central pillar of Ireland and the EU's decarbonisation strategy is focused on electrification of the transport fleet. In the first instance this drives a requirement for vehicle charging infrastructure and a consequent significant increase in electricity demand. A viable further consequence of this transformation is the potential for the electricity network to leverage these vehicle batteries when they are connected to the system via charging infrastructure. Technologies that can provide bi-directional (i.e. both charge an electric vehicle and extract charge for injection back into the grid) are known as Vehicle to Grid (V2G) chargers. Unit costs for such devices have fallen rapidly in line with increasing levels of EV deployment and there is an expectation that V2G functionality will be built directly into vehicles if monetization of their services is achieve.

3.4.1.2 Infrastructure Deployed

Figure 10 V2G Charger Infrastructure

The RESERVE Field Trial V2G Charger installation is located at the ESB offices in Leopardstown Dublin. It is the first known V2G installation located in Ireland. The device itself is rated at 10 kVA for both charging and discharging and connect to EVs over the CHAdeMO charging protocol. The installation was designed with a large interface kiosk (which can be seen on the left of the above image) which has allowed for collaborative use of the device with the Horizon 2020 SUCCESS project. The Field trial location sees throughput of EVs during the working week (Monday – Friday) but vehicles are never present at evenings or weekends. Given this could limit the scale and scope of testing for the RESERVE project a Nissan Leaf EV has been procured in order to provide continued dedicated access to a battery. Installation of the V2G Charger and associated infrastructure was completed in Q2 2018.

3.4.1.3 Communications

An edge computing device (Raspberry Pi) is connected to the Charge Point via ethernet to allow communication between the two devices. To receive readings from the Charge Point the Pi must request it. A script that is running on the Pi sends a request at a set time-interval. Upon receiving the readings, the Pi will use the locally running version of the AVM to calculate the Power Factor before the calculated value is sent back to the Charge Point.

While the Pi uses ethernet to communicate to the V2G Charge Point, a Wifi connection to a mobile network is required to communicate to the central cloud based AVM. The purpose for this connection is to enable to ability to update both the locally stored VVC and AVM software.

A user adds or updates a VVC by uploading it to the cloud hosted AVM in a JSON format. It is then stored in a database where it can only be accessed by the AVM. When a VVC is updated, the Raspberry Pi is notified and then sends an update request to the cloud based AVM, it should then receive a new VVC for it to use.

3.4.1.4 Data Information Systems & Software

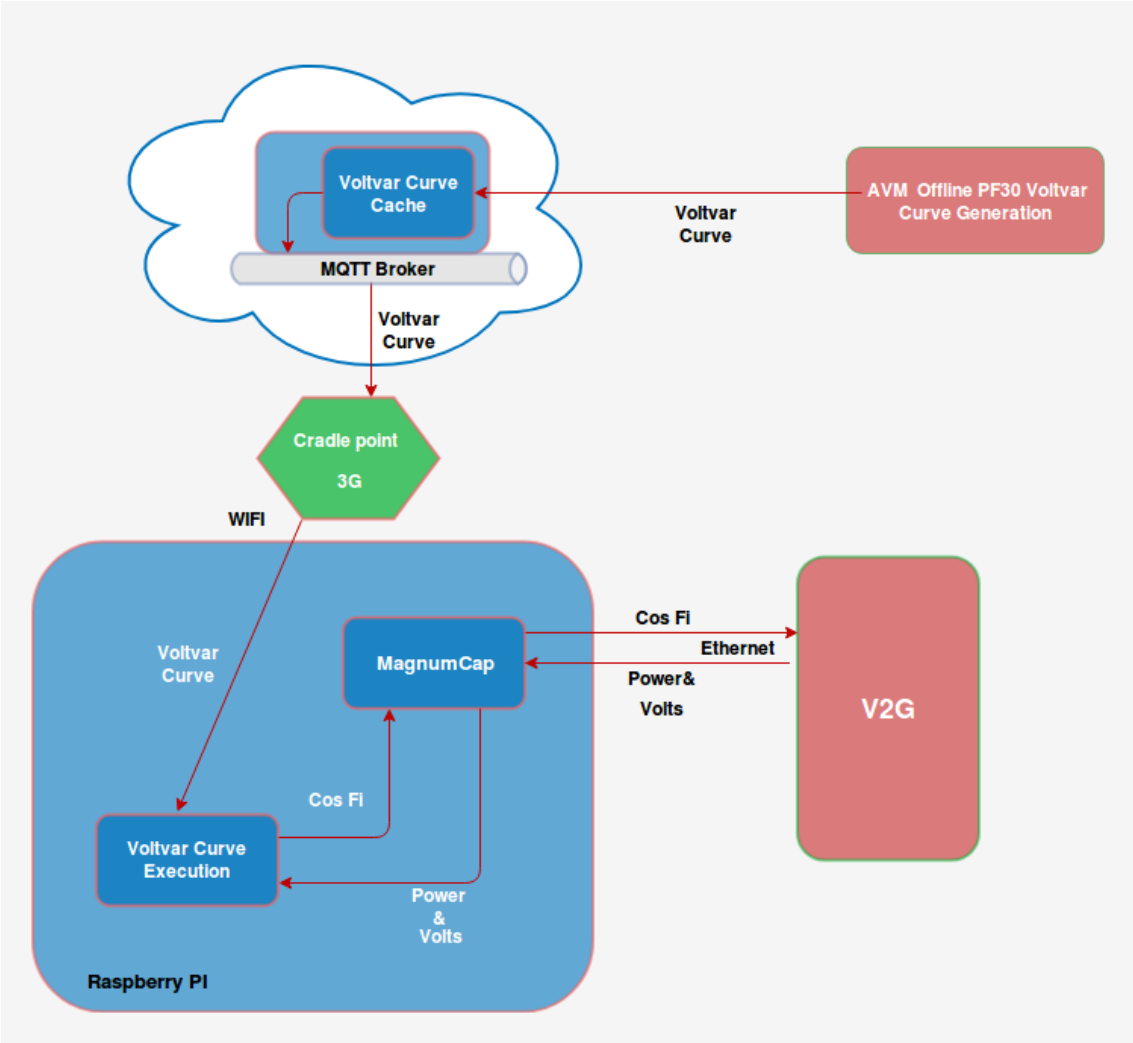

Figure 11 V2G AVM Execution Diagram

The VVC is initially stored within the cloud server and is then sent in a JSON format to the Raspberry Pi upon request, where it is then stored as a simple JSON file that can be read by the AVM. A Raspberry Pi 3 model B is used for this particular trial site. MQTT is used to communicate between the Pi and the cloud server and uses TLSv1.2 to encrypt the payloads. The communication between Pi and Charge Point is not encrypted as these messages are sent over a private ethernet connection. The Raspberry Pi itself is stored within a secured cabinet next to the Charge Point. This is to prevent any tampering with the hardware and to protect it from various weather conditions.

3.4.1.5 Tuning of AVM Algorithm to Specific Site

3.4.1.5.1 Input data and assumptions for V2G test site

Figure 11 shows the single-line diagram of a small feeder connected to the upstream system at Leopardstown for V2G charger installation. The batteries of the electric vehicles are connected using a three-phase inverter at V2G charge point. The battery power injection capacity is assumed to be 3 kW for each electric vehicle. The inverter capacity is considered to be 9 kVA. This inverter is a three-phase inverter. Therefore, minimisation of the voltage unbalance cannot be considered here as an objective.

It should be noted that V2G systems typically consume active power, except for the systems for which both operation strategies and technical characteristics of the charging station allow battery discharge. The owners of the electric vehicles may also raise an argument about discharging their vehicles' batteries in the course of time that they left their vehicles to be charged. In other words, the interface between the distribution grid and the EVs, instead of using typical power converters that only work on unidirectional mode, needs to use bidirectional power converters to charge the batteries (G2V - Grid-to-Vehicle mode) and to deliver part of the stored energy in the batteries back to the power grid (V2G - Vehicle-to-Grid mode). Usage profiles should be defined and controlled by a collaborative broker, taking into account the requirements of the low voltage distribution systems and the conveniences of the vehicle owners. In this section, it has been assumed that the charging station only consumes active power. However, reactive power can be easily exchanged between the V2G system and the grid.

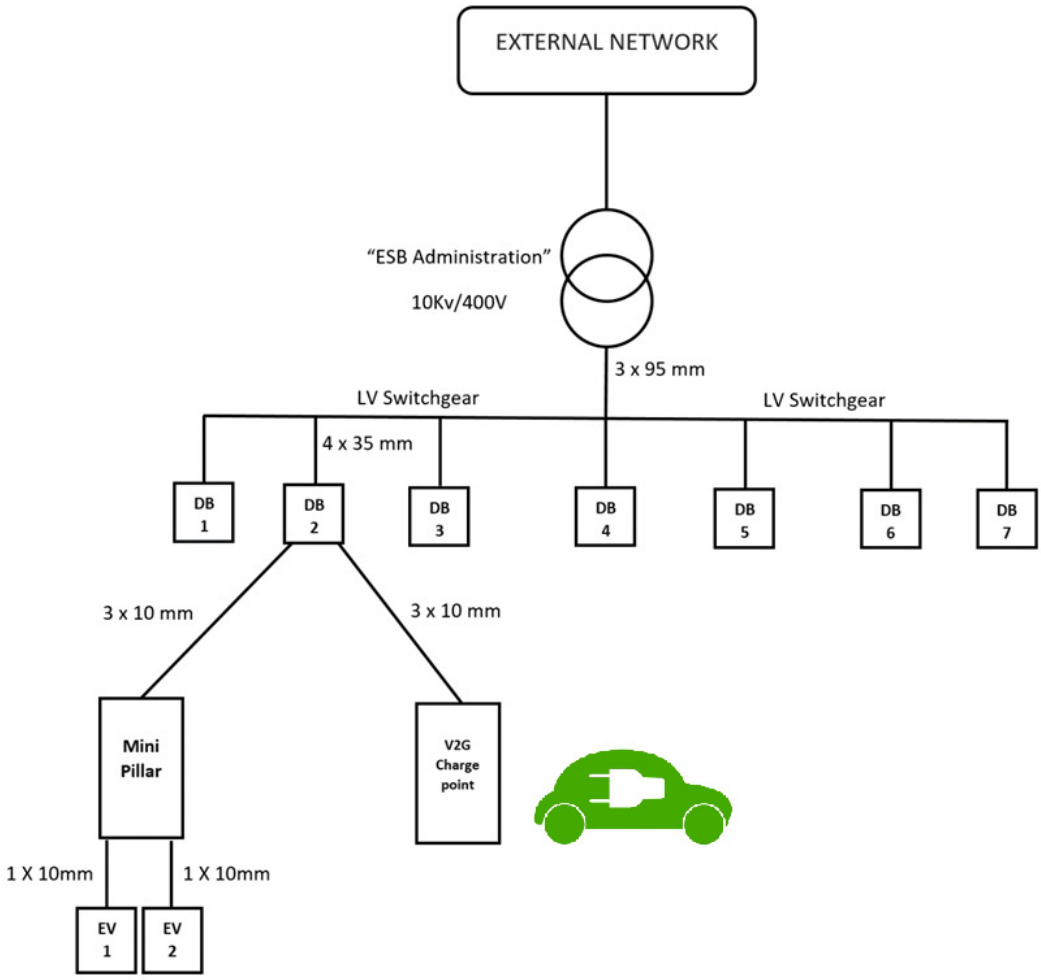

Figure 12 Single-line diagram of the small feeder at Leopardstown (trial site RES-V2G-LEOP-0) for V2G charger installation.

Fehler! Verweisquelle konnte nicht gefunden werden. gives the scenarios. In this table, P_{V2G} is the power injected to the system at PCC by the V2G charger. Coefficients of the ZIP load model are given by Z, I and P, for constant impedance, constant current and constant power components, respectively. Power Factor (PF) at the system load points is presented in Fehler! Verweisquelle konnte nicht gefunden werden. for different scenarios. The load has an unbalance distribution on phases (a), (b) and (c) at all load points (DB 1 to DB 7). Similar to two previously discussed trial sites Fehler! Verweisquelle konnte nicht gefunden werden. shows how

to calculate the active and reactive power demands on phase (a). The active and reactive power consumptions on other phases can be found similarly.

Scenario	Load Factor	P_{V2G} /S_{V2G}	Z	I	Power Factor	Un_a (%)	Un_b (%)	Un_c (%)
1	0.7	-0.1429	0.400	0.200	0.900	10.36	-10.4	2.95
2	0.6	0.0000	0.400	0.200	0.850	-10.3	9.6	2.19
3	0.5	0.0000	0.200	0.300	0.860	11.48	-9.67	1.03
4	0.5	-0.2857	0.200	0.300	0.870	9.25	-9.92	1.75
5	0.5	0.0000	0.300	0.250	0.870	-9.4	9.6	0.32
6	0.6	-0.4286	0.300	0.200	0.850	9.52	-9.67	2.72
7	0.6	0.0000	0.400	0.200	0.860	-10.17	10.64	2.64
8	0.7	-0.1429	0.400	0.200	0.870	11.49	-10.74	2.45
9	0.8	-0.2857	0.400	0.200	0.860	-11.41	9	0.78
10	0.75	-0.2857	0.300	0.250	0.880	9.18	-10.66	1.78
11	0.8	-0.2857	0.500	0.100	0.860	10.2	-10.93	0.07
12	0.8	0.0000	0.400	0.100	0.870	-10.58	9.88	1.28
13	0.8	-0.4286	0.400	0.200	0.880	10.25	-9.24	0.94
14	0.8	-0.5714	0.400	0.200	0.890	10.97	-9.66	0.48
15	0.8	-0.4286	0.500	0.150	0.900	-10.88	10.62	0.54
16	0.8	-0.5714	0.550	0.250	0.900	9.88	-10.26	1.27
17	0.8	-0.4286	0.400	0.200	0.910	-10.29	10.08	0.28
18	0.85	-0.5714	0.400	0.200	0.930	9.05	-9.04	1.8
19	0.9	-0.5714	0.450	0.200	0.910	-11.95	10.69	1.41
20	0.85	-0.4286	0.400	0.200	0.930	9.5	-9.29	2.09
21	0.88	-0.4286	0.450	0.200	0.940	-9.32	9.71	2.1
22	0.9	0.0000	0.400	0.200	0.920	10.12	-10.25	1.92

23	0.9	-0.2857	0.450	0.200	0.930	-9.59	10.62	0.1
24	0.85	-0.2857	0.400	0.200	0.950	-10.47	10.14	0.21
25	0.85	0.0000	0.400	0.100	0.930	10.02	-10.04	0.96
26	0.9	-0.1429	0.500	0.150	0.930	-11.85	10.76	1.59
27	0.95	-0.4286	0.500	0.200	0.940	11.76	-9.82	1.96
28	1	0.0000	0.600	0.100	0.930	-9.16	10.55	1.22
29	1	-0.2857	0.650	0.100	0.930	11.21	-10.23	2.46
30	0.9	-0.2857	0.700	0.100	0.960	-9.81	9.83	2.16
31	0.9	-0.1429	0.600	0.200	0.950	10.27	-10.5	2.91
32	0.95	0.0000	0.750	0.050	0.950	-10.64	10.42	1.59
33	0.8	-0.2857	0.600	0.200	0.940	11.83	-9.77	0.98
34	0.8	0.0000	0.750	0.050	0.930	-10.25	10.47	0.32
35	0.75	-0.2857	0.600	0.200	0.920	11.95	-9.35	1.83

Table 3 Scenarios for V2G Leopardstown

Phase a		Phase b		Phase c	
P^{max} (kW)	Q^{max} (kvar)	P^{max} (kW)	Q^{max} (kvar)	P^{max}(kW)	Q^{max} (kvar)
2.2	0.75	2.2	0.75	2.2	0.75

Table 4 Maximum Load on each phase at each load point (DB 1 to DB 7)

3.4.1.5.2 VVCs of the network RESs for minimisation of the voltage unbalance

With a three-phase inverter, the voltage unbalance cannot be effectively improved in distribution systems. The reason mostly lies under the fact that each phase of the three-phase controllable devices cannot be controlled separately and a single control unit provides the gate pulses for the inverter switches. Therefore, this inverter cannot be used to optimise the voltage unbalance in this network.

3.4.1.5.3 VVCs of the network RESs for minimisation of the total loss

The only controllable RES in this simple system is a three-phase V2G system. In this subsection the second objective function is considered in order to apply the proposed active voltage management algorithm and extract the VVC in this trial site. The final VVC for the V2G system as the only controllable device is presented in **Figure 12**

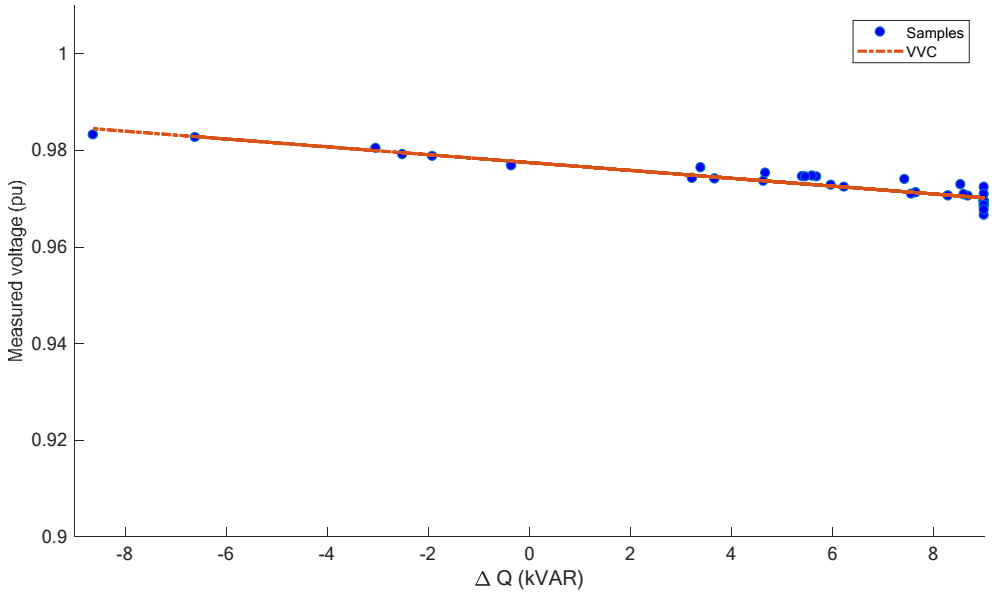

Figure 13 VVC of the new PV array for loss minimisation (m= -0.0008132 (pu/kvar), c= 0.977487 (pu), V_{opt}=0.977445 (pu)).

3.4.1.5.4 VVCs of the network RESs for minimisation of the voltage deviation from $V_{desired}$=1 pu at load points (DB 1 to DB 7)

Considering the third objective function for extracting the VVCs using the proposed active voltage management algorithm in this trial site, the AVM algorithm suggests that this inverter should inject its maximum reactive capacity in all possible scenarios. Therefore, no VVC can be found for this system with this objective. It should be noted that in every possible scenario, the active power production of each RES is determined by the availability of the regarding source, e.g., solar radiation and wind.

3.4.1.5.5 Summary of VVCs for this trial site

As discussed before, if the VVC proposes a reactive power support beyond the inverters' upper or lower limits, the reactive power support is set to the adjacent limit.

Table 5 summarizes the VVCs for this trial site. It should be noted that these VVCs are extracted assuming all the inverters working under power control mode of operation. For voltage control mode of operation, a voltage is proposed for each converter and of course for each objective. **Table 5** also presents such voltage levels.

	Reactive power control mode		**Voltage control mode**
	m (pu/kvar)	**c (pu)**	**V_{opt}**
Voltage Unbalance	NA	NA	NA
Energy Loss	-0.0008132	0.977487	0.977445
Voltage Deviation	NA	NA	1.00372

Table 5 VVC for the V2G system in both modes of operation for RES-V2G-LEOP-0

3.4.2 Solar Photovoltaic (PV) Array

3.4.2.1 Background

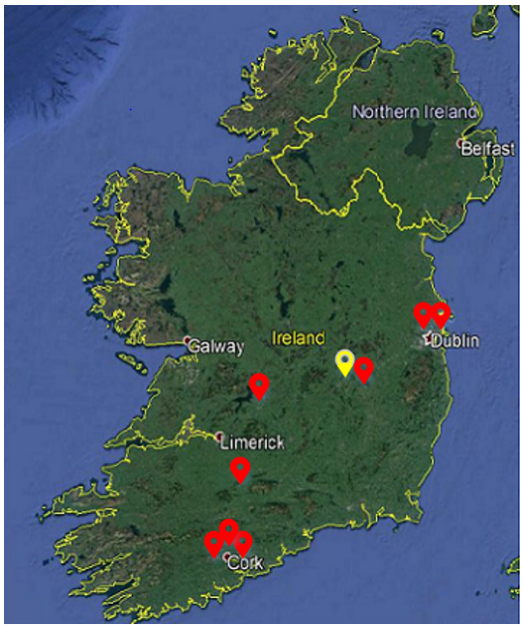

Figure 14 Location of Solar PV Array Trial Site

Of the inverter based technologies which are part of the RESERVE AVM Field Trials, Solar PV Arrays are possibly the most mature. There are in excess of 400 GW of Solar PV generation deployed globally which provides a very significant footprint for the realization of voltage control services. In line with this level of market maturity, techniques for communication with and the control of 'smart' inverters associated with PV installations are quite advanced. Examples include the Sunspec Alliance's Modbus interface for the control of Smart Inverters and California Energy Commission's Rule 21 governing rules for the interconnection of PV. The rate of deployment of Solar PV arrays in Ireland has lagged behind international norms but the recent announcement of the first national Support Scheme to specifically target Solar PV deployment is likely to yield increased levels of deployment.

3.4.2.2 Infrastructure Deployed

Figure 15 Solar PV Array in NTC, Portlaoise

The RESRVE AVM Solar PV Array Trial Site is located at the ESB's National Training Centre in Portlaoise, Co Laois. It comprises a 7.2 kW Ground Mounted Solar PV Array connected via two independent single phase inverters. The system is fully operational following the completion of installation and commissioning of the array in Q1 2018. Ongoing monitoring of the arrays' performance in the intervening period has created a baseline of data which will be used to assess the impact of the AVM technique on electricity generation capacity.

3.4.2.3 Communications

The Solar PV site, from an ICT perspective, is considered as a decentralised architecture in that the execution of the Volt-VAR curve is carried out at the edge and not in a central controller. While the central controller is required as a service tasked with the issuing of the VVC to the PV Unit for execution it plays no part in its actual execution from the perspective of calculating a set point value.

The communication between the central controller and the Solar PV unit will serve the purpose of sending the Volt-VAR curve points to the Solar PV unit. This communication will be enabled via the use of a preinstalled SMA Cluster Controller that exposes a gateway using a designated IP address and port. This gateway operates on a set of Modbus registers that allow the sending of control messages to the inverter. This gateway will be accessed from the central controller over TCP/IP and by OpenFMB (Open Messaging Field Bus) using the OpenFMB Modbus interface and broker to send the data to the relevant registry on the SMA Cluster Controller.

3.4.2.4 Data Information Systems & Software Implementation

Given that the SMA inverter can store and execute the Volt-VAR curve without intervention there is no requirement for any software to be installed on or at the inverter to execute the Volt-VAR curve. The inverter receives the VVC over 24 Modbus registries with each register representing a point value on the curve. For example an x value will be in one registry followed by a y value in the next. This will allow for 12 full curve points to be installed on the inverter.

Given that the VVC is currently stored in a JSON format there will be a software component required to convert the values to Modbus prior to sending them via OpenFMB to the SMA Cluster Controller gateway that will configure the inverter with the values.

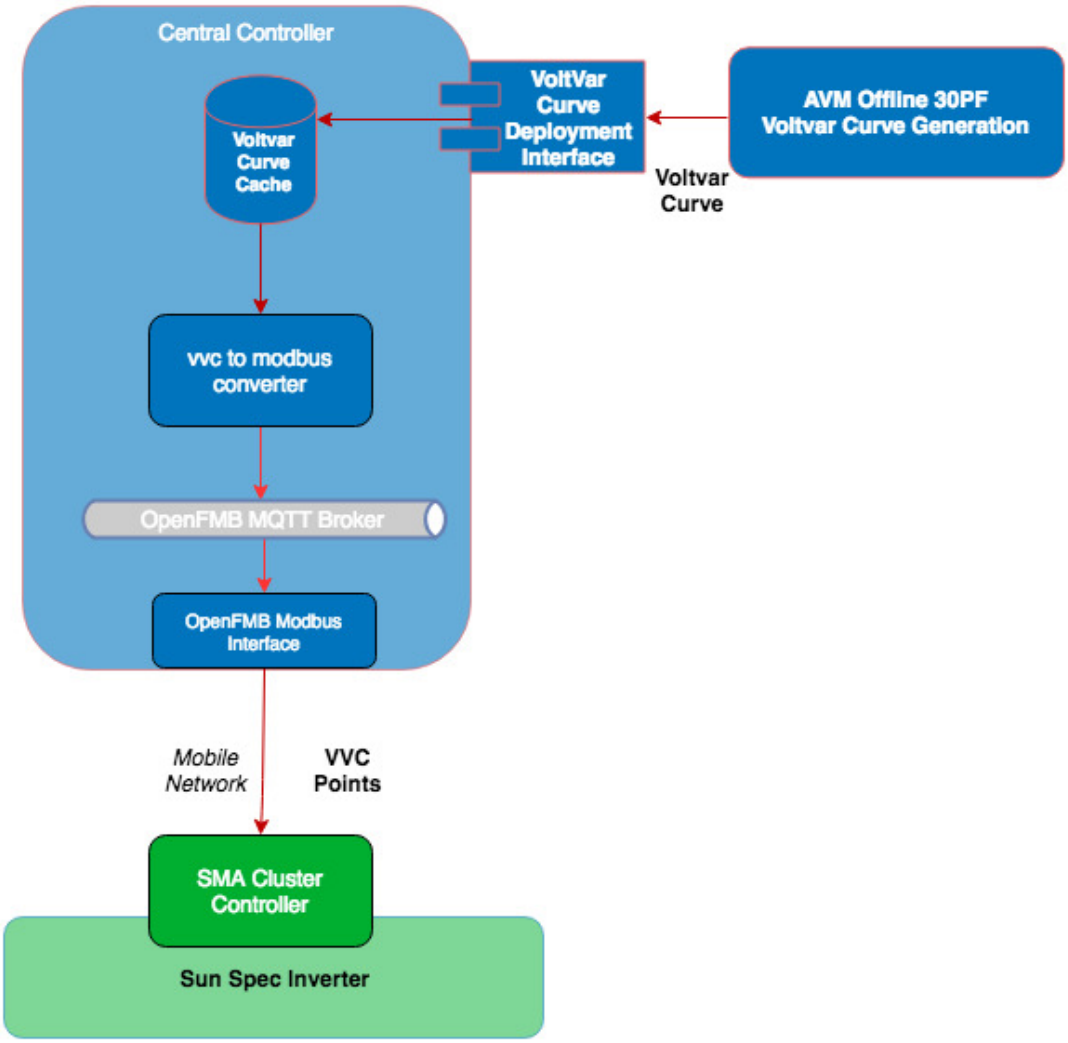

Figure 16 Solar PV AVM Execution Diagram

3.4.2.5 Tuning of AVM Algorithm to Specific Site

Figure 16 shows the single-line diagram of a small low voltage distribution system connected to the upstream system at Portlaoise. Different Renewable Energy Sources (RESs) including two PV arrays and a wind turbine are connected to this system at different connection points. Only the new PV array has a controllable inverter, and the other RESs are assumed to work at a fixed power factor (0.95 lagging). Due to the lack of enough data, some assumptions have been made. In **Figure 16**, some of these assumptions are distinguished in red.

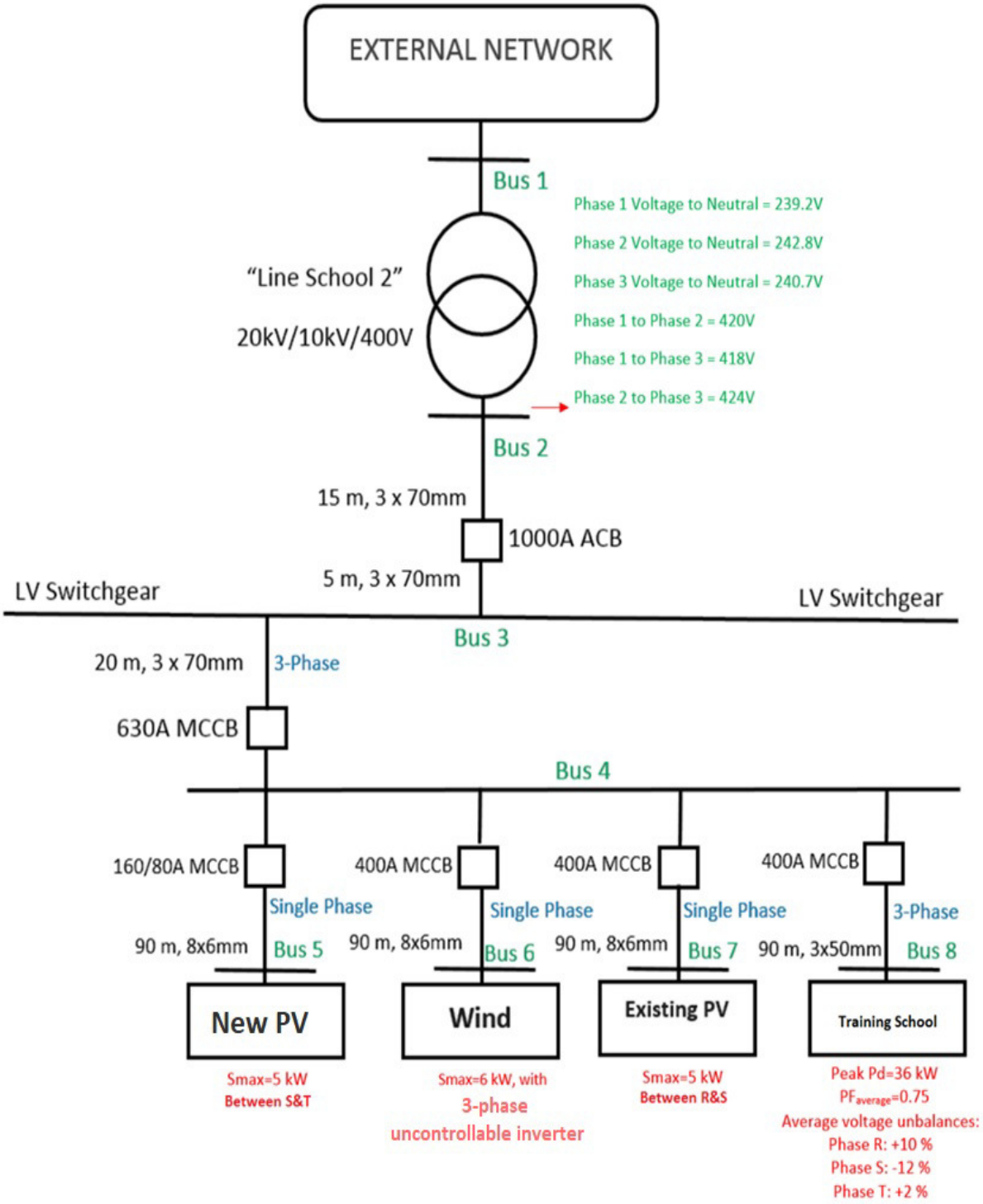

Figure 17 Single-line diagram of the small feeder at Portlaoise (trial site RES-PV-NTC-0) for RES installation.

Scenario	Load Factor	Z	I (P=1-Z-I)	Power Factor	Un_a (%)	Un_b (%)	Un_c (%)	$P_{existing}/S_{existing}$	P_{wind}/S_{wind}	P_{new}/S_{new}
1	0.7	0.4	0.2	0.9	10.36	-10.4	2.95	0	0	0
2	0.6	0.4	0.2	0.85	10.3	-9.6	2.19	0	0.25	0
3	0.5	0.2	0.3	0.86	11.48	-9.67	1.03	0	0.5	0
4	0.5	0.2	0.3	0.87	9.25	-9.92	1.75	0	0.75	0
5	0.5	0.3	0.25	0.87	9.4	-9.6	0.32	0	0.75	0
6	0.6	0.3	0.2	0.85	9.52	-9.67	2.72	0	0.5	0
7	0.6	0.4	0.2	0.86	10.17	-10.64	2.64	0	0.5	0
8	0.7	0.4	0.2	0.87	11.49	-10.74	2.45	0.25	1	0.5
9	0.8	0.4	0.2	0.86	11.41	-9	0.78	0.5	0.75	0.5
10	0.75	0.3	0.25	0.88	9.18	-10.66	1.78	0.25	0.5	0.5
11	0.8	0.5	0.1	0.86	10.2	-10.93	0.07	0.5	0.25	0.75
12	0.8	0.4	0.1	0.87	10.58	-9.88	1.28	0.5	0	0.5
13	0.8	0.4	0.2	0.88	10.25	-9.24	0.94	0.5	0.25	0.75
14	0.8	0.4	0.2	0.89	10.97	-9.66	0.48	1	0.25	1
15	0.8	0.5	0.15	0.9	10.88	-10.62	0.54	0.75	0.25	0.75
16	0.8	0.55	0.25	0.9	9.88	-10.26	1.27	1	0.25	0.75
17	0.8	0.4	0.2	0.91	10.29	-10.08	0.28	0.75	0.5	0.75
18	0.85	0.4	0.2	0.93	9.05	-9.04	1.8	1	0.5	1
19	0.9	0.45	0.2	0.91	11.95	-10.69	1.41	1	0.25	1
20	0.85	0.4	0.2	0.93	9.5	-9.29	2.09	0.75	0	0.5
21	0.88	0.45	0.2	0.94	9.32	-9.71	2.1	0.75	0.25	0.75
22	0.9	0.4	0.2	0.92	10.12	-10.25	1.92	0.5	0.5	0.5
23	0.9	0.45	0.2	0.93	9.59	-10.62	0.1	0.5	0.5	0.5
24	0.85	0.4	0.2	0.95	10.47	-10.14	0.21	0.5	0.5	0.75

25	0.85	0.4	0.1	0.93	10.02	-10.04	0.96	0.75	0.5	0.75
26	0.9	0.5	0.15	0.93	11.85	-10.76	1.59	0.25	0.75	0.5
27	0.95	0.5	0.2	0.94	11.76	-9.82	1.96	0.25	0.5	0.25
28	1	0.6	0.1	0.93	9.16	-10.55	1.22	0	0.75	0
29	1	0.65	0.1	0.93	11.21	-10.23	2.46	0	0.75	0
30	0.9	0.7	0.1	0.96	9.81	-9.83	2.16	0	0.5	0
31	0.9	0.6	0.2	0.95	10.27	-10.5	2.91	0	1	0
32	0.95	0.75	0.05	0.95	10.64	-10.42	1.59	0	0.75	0
33	0.8	0.6	0.2	0.94	11.83	-9.77	0.98	0	0.5	0
34	0.8	0.75	0.05	0.93	10.25	-10.47	0.32	0	0.25	0
35	0.75	0.6	0.2	0.92	11.95	-9.35	1.83	0	0	0

Table 6 Trial site Solar PV NTC

Table 4 gives the operation scenarios. In this table, P_{new}, P_{wind}, and $P_{existing}$ are the power injected by the new photovoltaic array, wind turbine and existing photovoltaic. Coefficients of the ZIP load model are given by Z, I and P, for constant impedance, constant current and constant power components, respectively.

Load Factor (LF) determines the ratio of the active power consumption and the maximum power consumption presented in **Table 7**. Power Factor (PF) is also presented in **Table 7**. This table also shows the load unbalance distribution on phases (R), (S) and (T) at the load point. Finally, Fehler! Verweisquelle konnte nicht gefunden werden. shows how to calculate the active and reactive power demands on phase (a). The active and reactive power consumptions on two other phases are found similarly.

Equation 1

$$P_{\mathrm{a},s} = P_{\mathrm{a}}^{\max}.\mathrm{LF}_s.(1+\mathrm{Un}_{\mathrm{a},s}/100)$$
$$Q_{\mathrm{a},s} = P_{\mathrm{a},s}.\mathrm{PF}_{\mathrm{s}}$$

Phase a		Phase b		Phase c	
Pmax (kW)	**Qmax (kvar)**	**Pmax (kW)**	**Qmax (kvar)**	**Pmax(kW)**	**Qmax (kvar)**

12	8	12	8	12	8

Table 7 Maximum Load on each phase at bus 8

3.4.2.5.1 VVCs of the network RESs for minimisation of the voltage unbalance

The only controllable RES in this simple system is the new solar array installed at bus 5 between phases S and T. Other two RESs (existing PV array and wind turbine) are not controllable. In this subsection the first objective function (**Table 2**) is considered in order to apply the proposed active voltage management algorithm and extract the VVC in this trial site. The VVC is presented in **Figure 17** for the new PV array. The slope and intercept of the VVC are given by m and c, respectively.

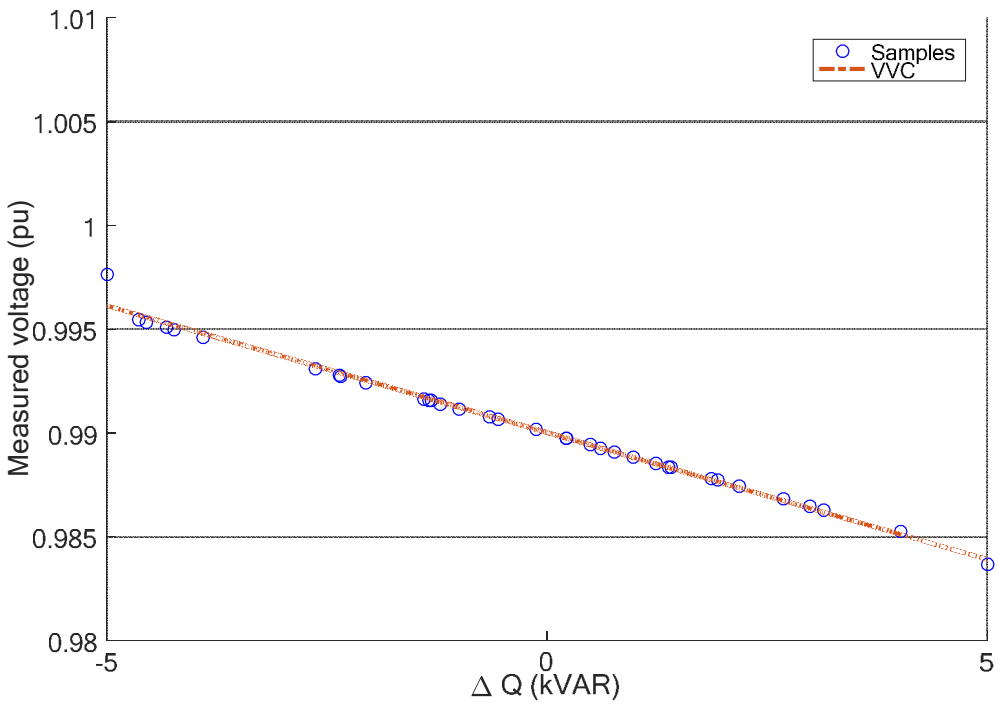

Figure 18 VVC of existing PV for voltage unbalance minimisation (m= -0.00122 (pu/kvar), c= 0.99002 pu).

3.4.2.5.2 VVCs of the network RESs for minimisation of total loss

The second objective is considered here to apply the active voltage management algorithm. The final VVC for the new PV array as the only controllable device is presented in **Figure 18.**

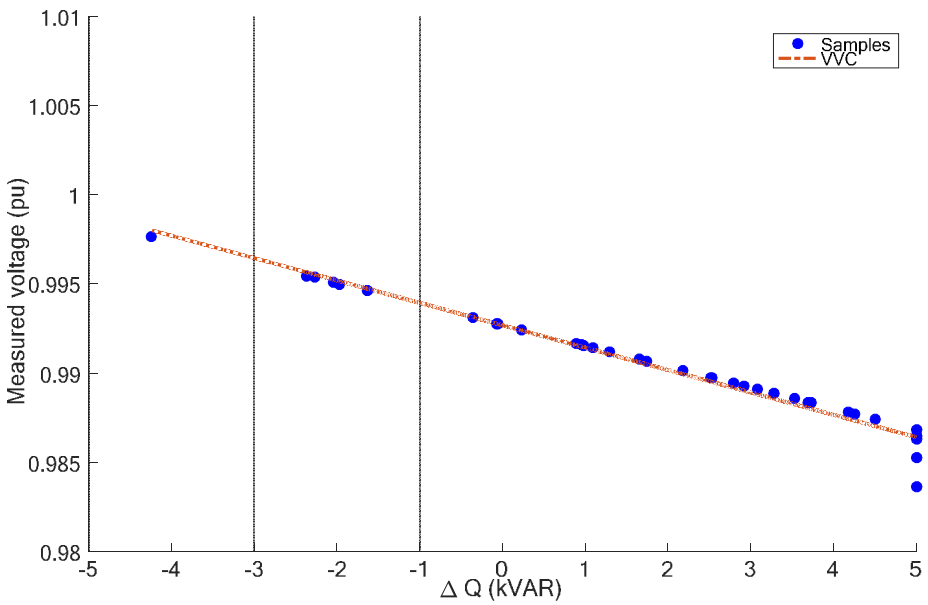

Figure 19 VVC of the new PV array for loss minimisation (m= -0.001254 (pu/kvar), c= 0.99268 (pu)).

3.4.2.5.3 VVCs of the network RESs for minimisation of the voltage deviation from $V_{desired}$=1 pu at load point (bus 8)

The third objective function is considered here for extracting the VVCs using the proposed active voltage management algorithm in this trial sites. In this case, the active voltage management algorithm suggests that all the inverters should inject their maximum reactive capacity.

It should be noted that in every possible scenario, the active power production of each RES is determined by the availability of the relevant source. For instance, the solar radiation determines the active power production of the system PV arrays. With the objective considered in this subsection, the inverters should fully dedicate their remaining capacities to provide positive reactive power support. As an example, if the active production of the new PV is 2 kW then this RES should inject 3 kvar reactive power (capacity of this RES is 5 kVA).

3.4.2.5.4 Summary of VVCs for this trial site

Objective	**Reactive power control mode**		**Voltage control mode**
	m (pu/kvar)	**c (pu)**	**V_{opt}**
Voltage Unbalance	-0.001221	0.99002	0.99005
Energy Loss	-0.001254	0.99268	0.99267
Voltage Deviation	NA	NA	1.01031

Table 8 VVC for the new PV array in both modes of operation

Finally, it should be noted that if the VVC proposes a reactive power support beyond the inverters' upper or lower limits, the reactive power support is set to the adjacent limit. **Table 8** summarizes the VVCs for this trial site. It should be noted that these VVCs are extracted with this assumption that all the inverters are operated under the reactive power control mode of operation. For voltage control mode, a voltage is proposed for each converter and of course for each objective. **Table 8** also gives these voltages.

3.4.3 Domestic Scale Battery Storage Sites

3.4.3.1 Background

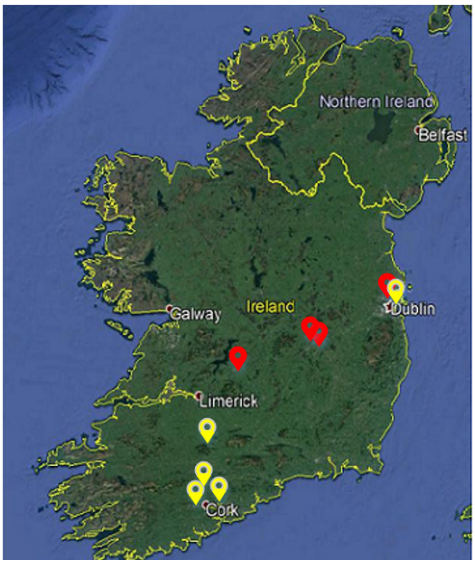

Figure 20 Locations of Domestic Scale Battery Storage Sites (Yellow Pins)

Due to the fact that electricity networks require instantaneous demand to be met by instantaneous generation the rise of intermittent renewable geneartion poses a complex problem. One potential solution to variable generation is the option of energy storage. Large-scale storage facilities have been in existance for many decades using technologies such a pumped hydro storage. The recent collapse in the unit cost of Lithium-ion batteris has resulted in small scale domestic scale storage installations becoming increasingly commercially viable. As such systems require inverter to convert from DC to AC they are another viable technology for the deplaoyment of the AVM control technique. Domestic scale battery system also provide additional use cases including price arbritage due to their ability to store electricity imported from the distribution network, allow the installation of increased small scale generation without the need to spill excess generation into the network as well as additional option for system services.

3.4.3.2 Infrastructure Deployed

Figure 21 Battery Storage System installed at a Rural Domestic Dwelling

A total of five sites have been selected for inclusion as Domestic Scale Battery Solution sites for Field Trials of the AVM control techniquie within RESERVE. The sites comprise a mixture of domestic, institutional and commercial premises located in both urban and rual settings, some with local small scale generation in place and each with a unique local distribution network configuration. A range of 10 - 12 kVA Li-Ion batteries has been installed at each of the locations. The diverse mixture of usage profiles at each of these locations coupled with the parallell engagment of a commercial aggregator in the opeartion of the battery systems will yield interesting results with regard to the benefit of the AVM control technique across a range of scenarios. AVM Control trials at the first Battery Storage site commenced in Q3 2018.

3.4.3.3 Communications

The architecture of this site is modelled on the Centralised System detailed in the D3.6 report which means that the execution of the Volt-VAR Curve (VVC) is carried out in a central location away from the inverter on site. The reason for choosing this centralised approach is due to the inverters at the site being behind an aggregator platform from which we communicate directly. This factor drives the communications requirements for this integration in terms of the technology used to transfer the data and protocol used for both entities to communicate. This communication is carried out over an SSL secured and encrypted MQTT broker to broker channel for both the receipt of the readings and the sending of the Reactive Power setpoint back to the RES Unit.

3.4.3.4 Data Information Systems & Software Implementation

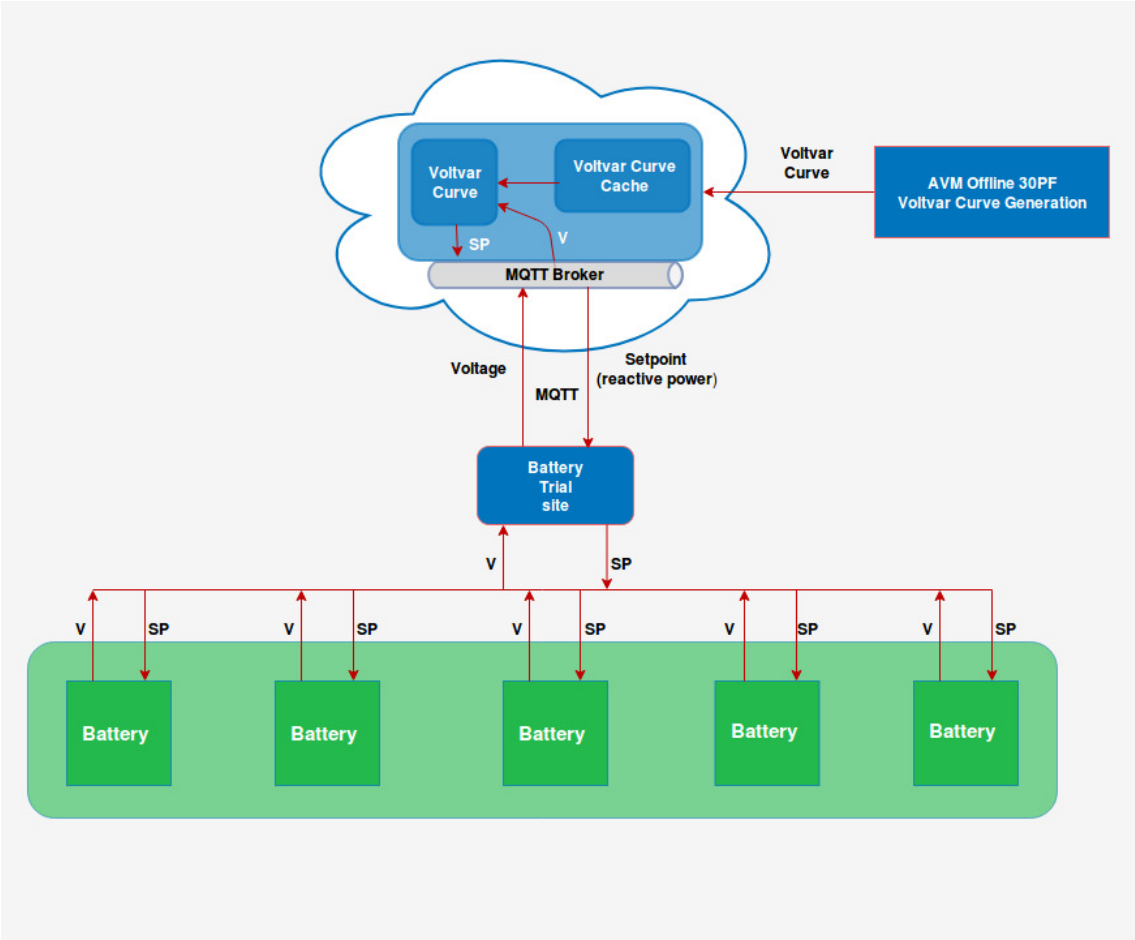

Figure 22 Battery Site AVM Execution Diagram

The diagram in Figure 22 demonstrates the components and data flow for the execution of the AVM technique on the Battery Trial Site. In this case the central cloud server contains components that are responsible for the receipt of the VVC from the AVM Offline 3-OPF application, the storage, the storage of that VVC, the receipt of the readings, the execution of the VVC and the subsequent sending of the setpoint back to the trial site. Each component with in the cloud server is built in a modular way and uses Docker as a containerisation tool to

The VVC objects are stored within a database hosted on the cloud server that only the AVM can access. The AVM itself is run within a Docker container on a Linux Server. The MQTT broker that both the trial site and AVM use to communicate is also hosted in the central cloud server. The communication between site and server is encrypted to ensure the messages are trustworthy.

3.4.3.5 Tuning of AVM Algorithm to Specific Site

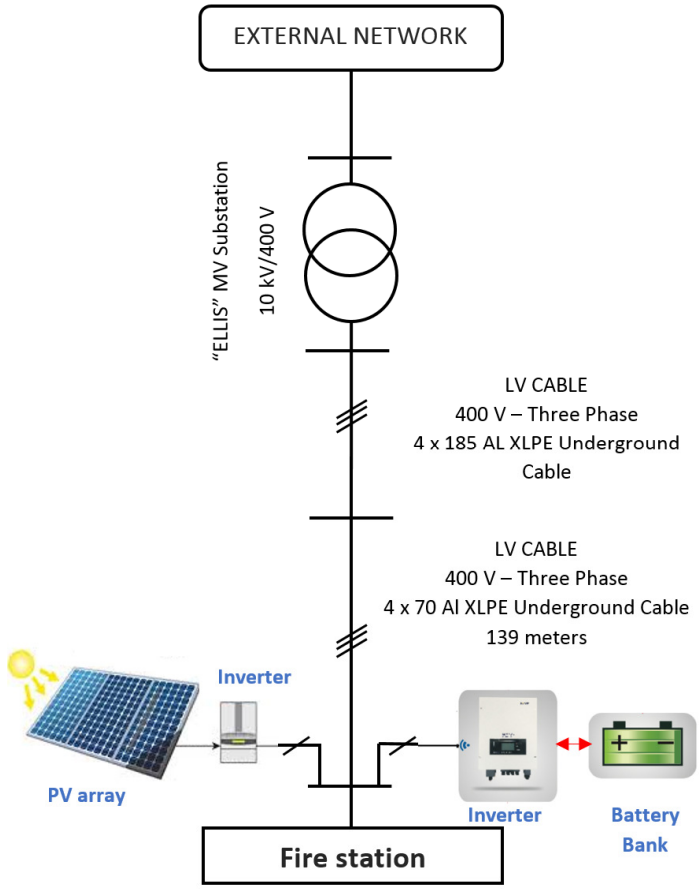

Figure 23 Single-line diagram of the small feeder at Ballyvolane for installation of the inverter-based controllable devices.

3.4.3.5.1 Input Data and Assumptions

Battery Storage	LG Chem Li-Ion 7kWh
Battery Inverter	Solar Edge AC Coupling Inverter SE3500, 3.5 kW
Solar PV Array	10.92 kW
Solar Inverter	SMA TriPower STP 9000TL-20, 9 kW

Table 9 DER present at Ballyvolane Fire Station

Figure 22 shows the single-line diagram of a small low voltage distribution system connected to the upstream system at Ballyvolane. A PV array, and a battery storage system with separate inverters are connected to this sample system. Characteristics of the inverters, solar array and battery are presented in **Table 9**. The solar PV array and battery storage system have been installed on phase (S).

Table 9 gives the system operation scenarios. In this table, P_{pv} and P_{bat} are the power production of the photovoltaic system and the battery, respectively. It is assumed that the photovoltaic and battery systems have been installed on phase (S). Coefficients of the ZIP load

model are given by Z, I and P, for constant impedance, constant current and constant power components, respectively. Coefficient P can be found using P=1-Z-I. Load Factor (LF) determines the ratio of the active power consumption and the maximum power consumption presented in. Power Factor (PF) is also presented in **Table 10**. **Table 10** also shows the load unbalance distribution on phases (a), (b) and (c) at fire station.

Scenario	Load Factor	P_{pv}/S_{pv}	P_{bat}/S_{bat}	Z	I	Power Factor	Un_a (%)	Un_b (%)	Un_c (%)
1	0.700	0.000	0.000	0.400	0.200	0.900	20.720	-2.800	4.425
2	0.600	0.000	-0.250	0.400	0.200	0.850	20.600	-1.200	3.285
3	0.500	0.000	-1.000	0.200	0.300	0.860	-10.960	19.340	-1.545
4	0.500	0.000	-0.750	0.200	0.300	0.870	0.500	29.840	2.625
5	0.500	0.000	-0.750	0.300	0.250	0.870	-18.800	37.200	-0.480
6	0.600	0.000	-0.500	0.300	0.200	0.850	3.040	6.660	4.080
7	0.600	0.000	-0.250	0.400	0.200	0.860	-20.340	29.280	-3.960
8	0.700	0.200	0.000	0.400	0.200	0.870	-22.980	39.480	3.675
9	0.800	0.400	0.000	0.400	0.200	0.860	18.820	0.000	-1.170
10	0.750	0.400	0.000	0.300	0.250	0.880	18.360	39.320	2.670
11	0.800	0.400	0.000	0.500	0.100	0.860	10.400	16.140	-0.105
12	0.800	0.400	0.000	0.400	0.100	0.870	21.160	-1.760	1.920
13	0.800	0.600	-0.250	0.400	0.200	0.880	0.500	42.480	-1.410
14	0.800	0.800	-0.250	0.400	0.200	0.890	-11.940	43.320	0.720
15	0.800	0.600	-0.250	0.500	0.150	0.900	21.760	-3.240	-0.810
16	0.800	0.800	-0.250	0.550	0.250	0.900	19.760	38.520	1.905
17	0.800	0.600	0.000	0.400	0.200	0.910	20.580	-2.160	-0.420
18	0.850	0.800	0.000	0.400	0.200	0.930	18.100	-0.080	2.700
19	0.900	0.800	0.000	0.450	0.200	0.910	-31.900	39.380	-2.115
20	0.850	0.600	0.000	0.400	0.200	0.930	19.000	-0.580	3.135
21	0.880	0.600	0.000	0.450	0.200	0.940	0.640	-1.420	-3.150
22	0.900	0.400	0.500	0.400	0.200	0.920	20.240	-2.500	2.880

23	0.900	0.400	0.250	0.450	0.200	0.930	19.180	-3.240	-0.150
24	0.850	0.600	0.000	0.400	0.200	0.950	0.940	-2.280	0.315
25	0.850	0.600	0.250	0.400	0.100	0.930	20.040	38.080	-1.440
26	0.900	0.200	0.250	0.500	0.150	0.930	23.700	-3.520	2.385
27	0.950	0.600	0.250	0.500	0.200	0.940	-19.520	37.640	-2.940
28	1.000	0.000	0.500	0.600	0.100	0.930	18.320	39.100	1.830
29	1.000	0.000	0.750	0.650	0.100	0.930	0.420	-2.460	-3.690
30	0.900	0.000	0.500	0.700	0.100	0.960	19.620	-1.660	3.240
31	0.900	0.000	0.750	0.600	0.200	0.950	20.540	39.000	-4.365
32	0.950	0.000	0.250	0.750	0.050	0.950	21.280	-2.840	2.385
33	0.800	0.000	0.250	0.600	0.200	0.940	3.660	14.460	-1.470
34	0.800	0.000	0.000	0.750	0.050	0.930	10.500	-0.940	0.480
35	0.750	0.000	0.000	0.600	0.200	0.920	23.900	36.700	-2.745

Table 10 Scenarios for RES-BAT-FIRE-0

Phase R		Phase S		Phase T	
P^{max} (kW)	Q^{max} (kvar)	P^{max} (kW)	Q^{max} (kvar)	P^{max}(kW)	Q^{max} (kvar)
15	7	15	7	15	7

Table 11 Maximum Load on each phase for RES-BAT-FIRE-0

3.4.3.5.2 VVCs of the network controllable devices for minimisation of the voltage unbalance

In this subsection, the first objective function (**Table 2**) is considered to apply the proposed active voltage management algorithm and extract the VVCs in this trial sites. These VVCs are presented in **Figure 23** and **Figure 24** for the PV array and battery storage bank, respectively. The slope and intercept of the VVC are given by m and c, respectively.

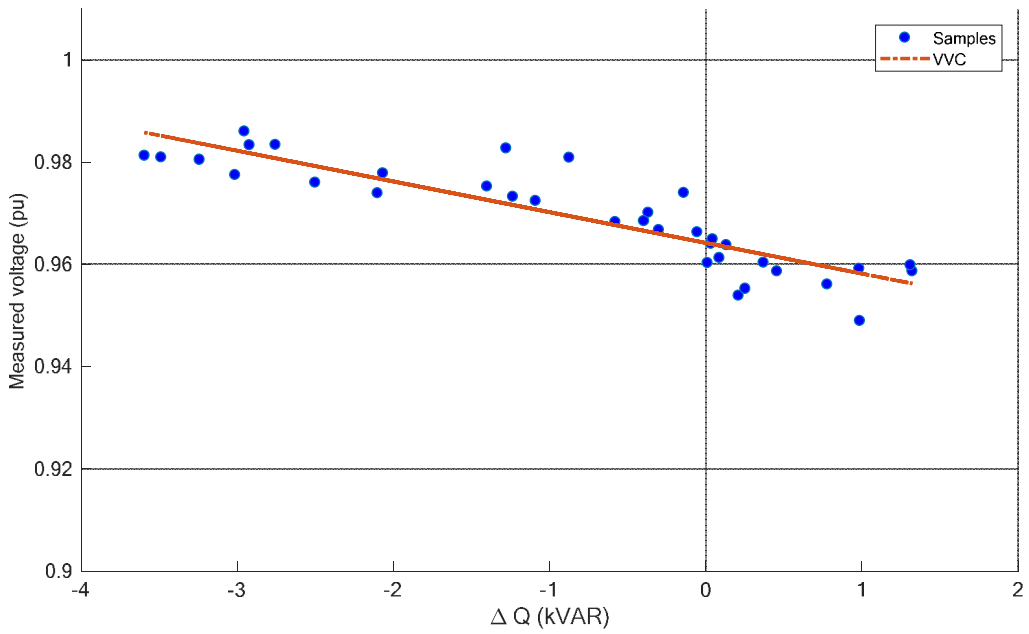

Figure 24 VVC of the PV array for minimisation of the voltage unbalance (m= -0.006014 (pu/kvar), c= 0.96520 pu, V_{opt}=0.965273).

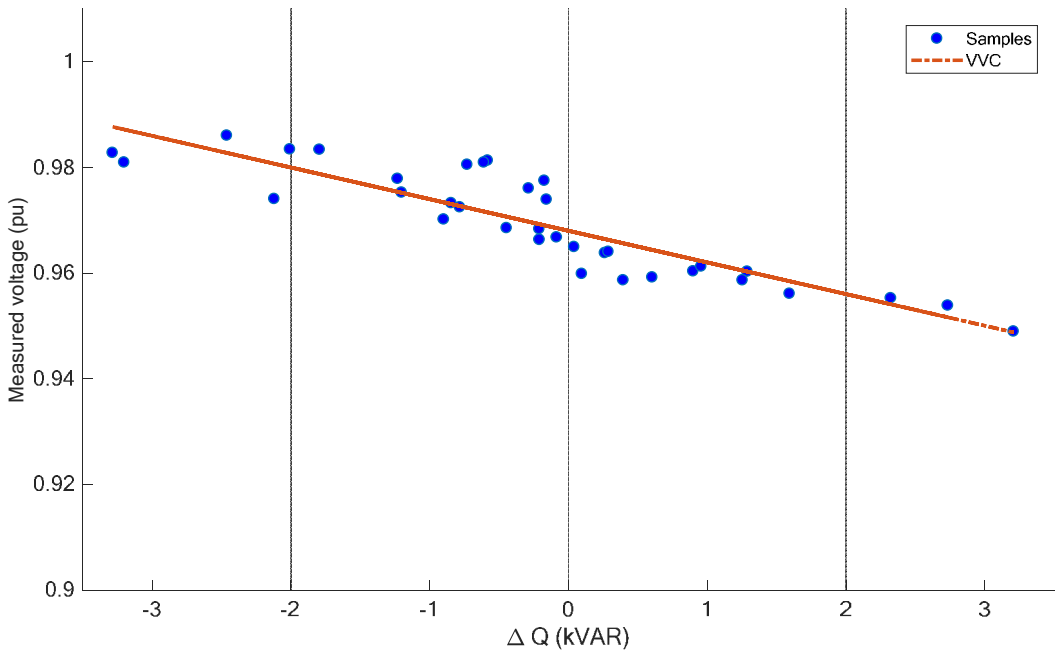

Figure 25 VVC of the battery storage for minimisation of the voltage unbalance (m= -0.00122 (pu/kvar), c= 0.96518 (pu), V_{opt}=0.965273 (pu)).

3.4.3.5.3 VVCs for the network RESs for minimisation of the total loss

The second objective is considered here in order to apply the AVM algorithm for this trial site. The final VVCs for the PV array and battery storage as the controllable device in this trial site are presented in **Figure 25** and **Figure 26**, respectively.

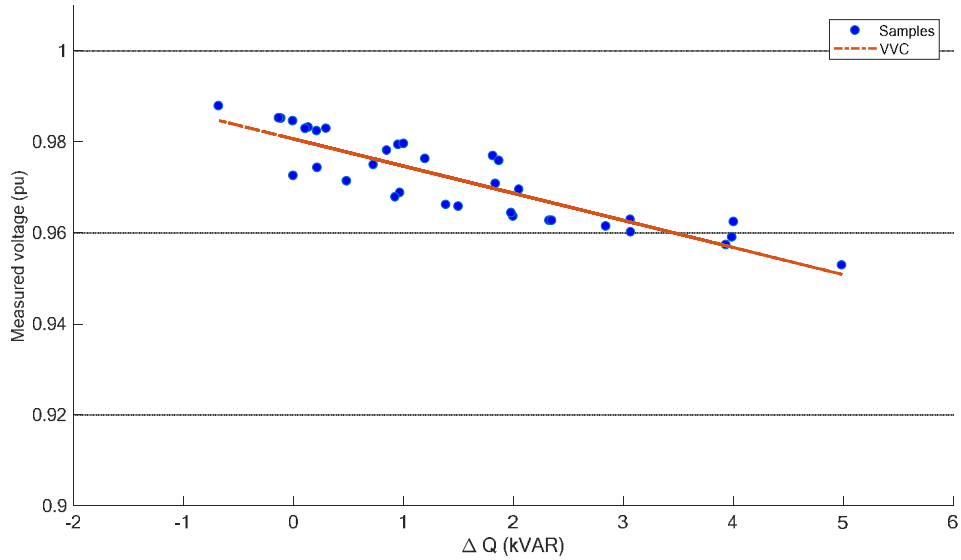

Figure 26 VVC of the PV array for loss minimisation (m= -0.005968 (pu/kvar), c= 0.98068 (pu), Vopt= 0.98243 (pu)).

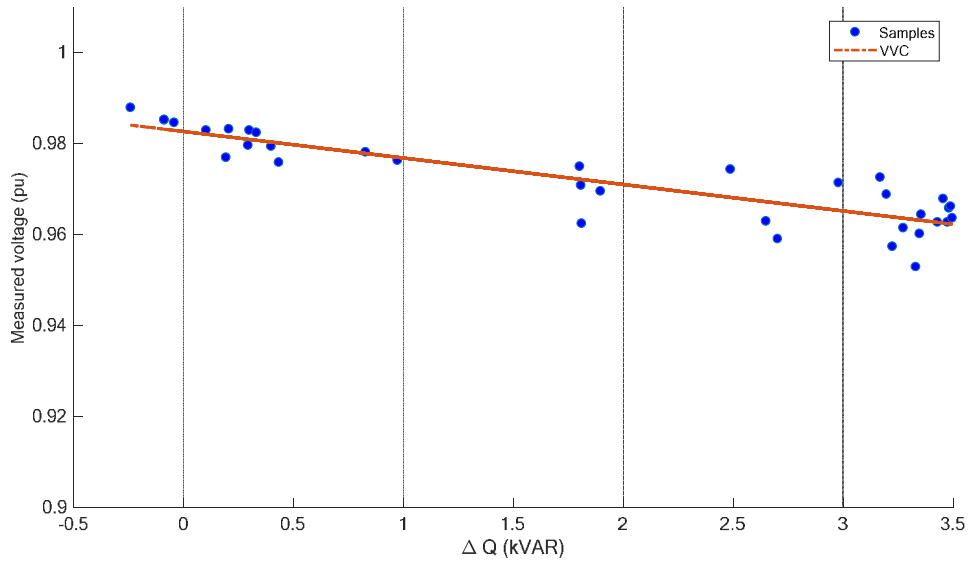

Figure 27 VVC of the battery storage for loss minimisation (m= -0.0058251 (pu/kvar), c= 0.982678 (pu), Vopt= 0.98243 (pu)).

3.4.3.5.4 VVCs for the network RESs for minimisation of the voltage deviation from $V_{desired}$=1 pu at load point (Fire Station)

The second objective function is considered here for extracting the VVCs using the proposed active voltage management algorithm in this study. For this trial site, the AVM algorithm suggests that all the inverters should inject the maximum available reactive capacity. It should be noted that in every possible scenario, the active power production of PV array and battery storage is determined by the availability of the corresponding source. With the objective considered in this subsection, the inverters should fully dedicate their remaining capacities to provide positive reactive power support.

3.4.3.5.5 Summary of VVCs for this trial site

	Reactive power control mode		Voltage control mode
	m (pu/kvar)	**c (pu)**	**V_{opt} (pu)**
Voltage Unbalance	PV: -0.006014 Battery: -0.00122	PV: 0.96520 Battery: 0.96518	PV: 0.965273 Battery: 0.965273
Energy Loss	PV: -0.005968 Battery: -0.0058251	PV: 0.98068 Battery: 0.982678	PV: 0.98243 Battery: 0.98243
Voltage Deviation	NA	NA	PV: 1.008932 Battery: 1.008932

Table 12 VVC characteristics for the PV array and battery storage in both modes of operation for RES-BAT-FIRE-0

Table 12 summarizes the VVCs for this trial site. It should be noted that these VVCs are extracted with this assumption that all the inverters are operated under reactive power control mode of operation. For voltage control mode, an optimal voltage level is proposed for each converter and of course for each objective. **Table 12** also gives these optimal voltages.

Finally, it should be noted that if a VVC proposes reactive power support beyond the inverters' upper or lower limits, the reactive power support is set to the adjacent limit.

3.4.4 Controllable Air Source Heat Pumps

3.4.4.1 Introduction

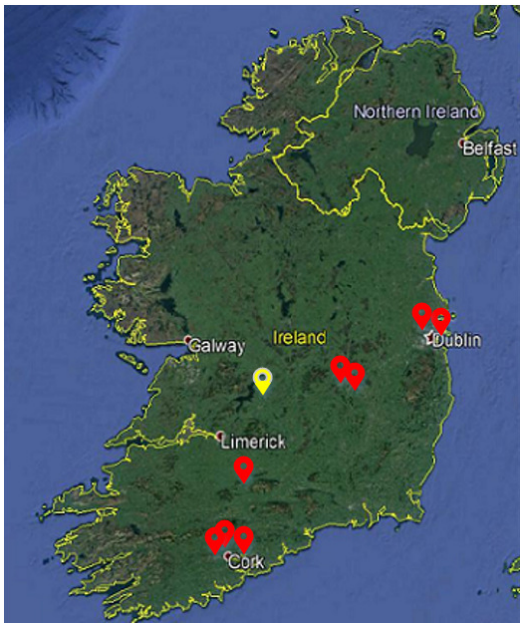

Figure 28 Location of ASHP Trial Site

A key pillar of Ireland's decarbonisation straegy is to shift the heating of buildings away from traditional fossil fuel based systems and towards electricfied heat (eHeat). The predominant technology for delivring eHeat is that of Air Source Heat Pump (ASHPs). All moderns ASHPs are inverter based and therefore have the potential to proivde system services to the distribution network through techinques such as those developed within the RESERVE project. A consequence of any shift towards eHeat is increased demand and stresses on the existing distribution network and an increase in the value of system services such as those provided by the AVM control techniique.

In identifying technolgies to field test the control techniques developed in RESRVE ASHPs were identified as one of specific relevance given the expected increase in deployments both nationally and internationally. A test site was identified (detailed in section 3.4.4.2 below) and engagement with ASHP OEMs took place. Intial feedback from these engagements was positive with OEMs recognising that provision of system services by means of their inverters could both create an additional revenue stream and also potentially assist in lowering network constraints that could inhibit extensive ASHP deployment. Despite these positive indications the OEMs were unfortunately not sufficiently comfortable to allow third party control of the ASHP inverters at this time but continue to be open to such engagements in the future. Given the potential significance of ASHP control combined with the progress made in identifying and developing a site it was decided to proceed with the ASHP field trial albeit using a somewhat simpler Demand Side Management (DSM) based control trial rather than the AVM inverter based trail originally planned.

3.4.4.2 Infrastructure Deployed

Figure 29 ASHP Units Installed at Youghalarra N.S.

A primary school located at Youghalarra N.S., Nenagh, Co Tipperary was identified as suitable field trial location for ASHPs. The school was undergoing a deep retrofit with significant improvements in insulation and air tightness being installed. It was decided to combine this fabric upgrade with a complete switch to eHeat through the installation of cascaded 14 kW ASHPs to provide all of the building's space & water heating. The cascaded design allows the installation to most efficiently match the heating requirements at any point in time due to the fact a single ASHPs minimum load is generally limited to 30% of its rated capacity. The switch to ASHP based heating necessitated a significant upgrade to the school's electrical supply to that of a 29 kVA LV capacity. All installation works were completed by end of Q2 2018.

3.4.4.3 Communications

Owing to the relatively simplified nature of the control scheme required for the operation of a DSM based control scheme it was decided to look at other options for testing new forms of technology within the RESERVE project. In particular the high latency, low bandwidth requirements of such a scheme make the deployment of a Low-Power Wide-Area Network (LPWAN) communications solution viable. This solution should provide learnings on the practicalities of integrating such a solution with a power system control scheme and could point to a low cost rapidly scaleable solution for the mass deployment of such devices. With this in mind a number of commercially available LPWAN based solutions are being assessed in order to determine the optimal deployment for this particular trial site.

3.4.5 Verification of Network Codes

The ability to verify the networks codes proposed in WP1 is limited by the capabilities of the currently commercially available inverter based technologies deployed and the permitted limits of network performance on Ireland's distribution networks.

Given these constraints two of the Network Codes proposed in D3.8 have been identified for testing at the field trial locations namely;

1. Reactive Power Capability of Distributed Generators

2. Decentralised Voltage Control

Analysis of the performance of the field trial with regard to these proposed new Network Codes will be conducted once initial trials of AVM performance have been completed.

In addition, efforts will continue to attempt to identify if alterations to the configuration of any of the trial sites will allow for the testing and verification of other Network Code proposals.

4. Conclusions

The development of Field Trail Infrastructure to facilitate the testing of the Voltage Control Concepts developed in the RESRVE projects remains broadly on track. All trial site deployments have been progressed sufficiently to allow for trails across field trial locations and technologies during the remaining 12 months of the project.

With regard to the testing the proposed DVSM technique, new class of inverters are currently under development. The first prototype of the measurement boards is currently under test and first tested prototype of the power and filter board will be completed by M26. The mapping between NCs with both simulation scenarios and field trials are completed. Few of the real time simulations are completed and remaining simulations are planned to be completed in the next 6 months.

With regard to field testing the AVM control technique a total of eight field trail locations have been developed which incorporate a diverse array of inverter based technologies. Site specific tuned implementations of the AVM technique (which present as tuned Volt-var curves) have been developed for all trial sites. ICT links for the monitoring of these sites and the implementation of the AVM control technique itself are at an advanced stage of development or deployment across all of these sites. Initial trials of the AVM technique in the field have commence at one of the Domestic Scale Battery sites which allows for the imminent assessment of performance. Further assessment of AVM performance across all sites continue during the coming months and will proceed to the investigation of the performance of a number of new Network Code Proposals on the trial site infrastructure.

5. List of figures

6. List of Tables

7. List of Abbreviations

ASHP	Air Source Heat Pump
AVM	Active Voltage Management
CHAdeMO	CHArge on de Move (A DC for Fast Charging Protocol for Electric Vehicles)
DVSM	Dynamic Voltage Stability Margin
ESB	Electricity Supply Board
FPGA	Field Programmable Gate Array
GIS	Gas Insulated Switchgear
HiL	Hardware in the Loop
ICT	Information & Communications Technology
LPWAN	Low-Power Wide-Area Network
MQTT	Message Queuing Telemetry Transport
N.S.	National (Primary) School
OPF `	Optimised Power Flow
OpenFMB	Open Field Message Bus
PRBS	Pseudo Random Binary Sequence
p.u.	per unit
PV	Photo-Voltaic
RWTH	Rheinisch-Westfälische Technische Hochschule
SSAU	Secondary Substation Automation Unit
V2G	Vehicle to Grid
VOI	Virtual Output Impedance
VVC	Volt-var Curve
WSI	Wideband System Identification